Hill-type computational models of muscle-tendon actuators: a systematic review

Arnault H. Caillet[1], Andrew T.M. Phillips[1], Christopher Carty[2,3], Dario Farina[4], Luca Modenese[1,5]

[1]Department of Civil and Environmental Engineering, Imperial College London, SW7 2AZ, UK

[2]Griffith Centre of Biomedical and Rehabilitation Engineering (GCORE), Griffith University, Australia

[3]Department of Orthopaedics, Children's Health Queensland Hospital and Health Service, Brisbane, Australia

[4]Department of Bioengineering, Imperial College London, SW7 2AZ, UK

[5]Graduate School of Biomedical Engineering, University of New South Wales, Sydney, Australia

Email: arnault.caillet17@imperial.ac.uk

NUMBER OF PAGES: 51

NUMBER OF FIGURES: 8

NUMBER OF TABLES: 4

NUMBER OF WORDS FOR ABSTRACT: 233

CONFLICT OF INTEREST STATEMENT: The authors declare no competing financial interests.

ACKNOWLEDGEMENTS: Skempton Scholarship to AC; Imperial College Research Fellowship to LM. LM also acknowledges support of the UNSW Scientia Fellowship scheme. The funders had no role in study design, data collection and analysis, decision to publish, or preparation of the manuscript.

Abstract

Backed by a century of research and development, Hill-type muscle-tendon models are extensively used for countless applications. Lacking recent reviews, the field of Hill-type modelling is however dense and hard-to-explore, with detrimental consequences on knowledge transmission, inter-study consistency, and innovation. Here we present the first systematic review of the field of Hill-type muscle-tendon modelling. It aims to clarify the literature by detailing its contents and proposing updated terminology and definitions, and discussing the state-of-the-art by identifying the latest advances, current gaps, and potential improvements in modelling muscle properties. To achieve this aim, fifty-five criteria-abiding studies were extracted using a systematic search and their Hill-type models assessed according to a completeness evaluation, which identified the modelled muscle-tendon properties, and a modelling evaluation, which considered the level of validation and reusability of the model, and attention given to its modelling strategy and calibration. It is concluded that most models (1) do not significantly advance the dated gold standards in muscle modelling and do not build upon more recent advances, (2) overlook the importance of parameter identification and tuning, (3) are not strongly validated, and (4) are not reusable in other studies. Besides providing a convenient tool supported by extensive supplementary material for understanding the literature, the results of this review open a discussion on the necessity for global recommendations in Hill-type modelling and more frequent reviews to optimize inter-study consistency, knowledge transmission and model reusability.

Introduction

Computational skeletal muscle-tendon (MT) models mimic the dynamics of muscle contraction by predicting the time profile of relevant muscle-related quantities that are challenging or impossible to obtain in vivo (Gollapudi & Lin, 2009; Dick et al., 2017; Monte et al., 2020; Zhang et al., 2021), including muscle force and fascicle length and velocity.

In the field of MT modelling, Hill-type models are globally more popular than other available solutions, such as analytical descriptions of the muscle twitch (Fuglevand et al., 1993; Ding et al., 2000; Frey Law & Shields, 2006), Huxley-type cross-bridge models (Huxley & Hanson, 1954; Huxley & Niedergerke, 1954; Julian, 1969; Zahalak, 1981; Smith et al., 2005; Lemaire et al., 2016), continuum models (Röhrle et al., 2012; Heidlauf et al., 2017; Röhrle, Oliver, Yavuz et al., 2019; Gfrerer & Simeon, 2021), and other comprehensive models (Tamura et al., 2008), for several reasons. With sarcomere-to-muscle multiscale simplifications and phenomenological modelling approaches, Hill-type models rely on fewer parameters and are computationally cheaper and conceptually simpler (Winters, J. M. & Stark, 1987; Lemaire et al., 2016; Hamburger, 2017; Schmitt et al., 2019) than Huxley-type or continuum models, while they are complex enough to describe the chain of neuromechanical events responsible for muscle force generation, which makes them more accurate, flexible and prone to further refinements (Schmitt et al., 2019) than analytical models. Hill-type models build upon a century of advancing research, a genesis of which is provided in Supplementary Material 1 (SM1), making it a reliable tool, the fair predictive accuracy of which has been extensively validated for various modelling variants, species, subjects, muscles and tasks. Hill-type models can also be used to receive experimental neural input such as bipolar (Hatze, 1980; Hof & Van den Berg, 1981; Zajac, 1989; Lloyd & Besier, 2003; Wakeling, James et al., 2012) and high-density (Sartori et al., 2017; Caillet et al., 2022) electromyograms (bEMG and HDEMG) or Functional Electrical Stimulation (FES) (Dorgan & O'Malley, 1997), and are embedded in user-friendly biomechanical simulation platforms, including for example

OpenSim (Delp, S. L. et al., 2007; Seth et al., 2018; Dembia et al., 2020) and AnyBody (Rasmussen et al., 2002; Rasmussen et al., 2003), which makes them more accessible in experimental data-driven musculoskeletal (MSK) investigations than other solutions. Hill-type models are therefore used in a wide range of applications, either (1) to investigate the muscle-tendon interplay (Zajac, 1989; Caldwell, 1995), muscle energetics (Houdijk et al., 2006; Ross, Ryan et al., 2018; Ross et al., 2020), contractile mechanics (Till et al., 2008; Bayer et al., 2017) and neuromechanics (Mörl et al., 2012) and age-related and neuromuscular impairment-related effects (Thelen, 2003; Shao et al., 2009; Hasson & Caldwell, 2011); (2) to explore motor control (Winters, Jack M. & Stark, 1985; Walter et al., 2014; Caggiano et al., 2022; Caillet et al., 2022), muscle reflex (Winters, J. M., 1995; Geyer et al., 2003; Geyer & Herr, 2010), and the response of the human body to perturbations (He J. | Levine W.S. | Loeb G.E., 1991; van Soest & Bobbert, 1993; John et al., 2013); (3) in MSK studies to assess the muscles' interactions with surrounding structures, such as the muscles' relative force contribution to joint torques, motion and contact forces (McLean et al., 2003; Shao et al., 2009; Nikooyan et al., 2012; Putra et al., 2015; Bicer et al., 2022), the indeterminacy of the load sharing system (Sarshari et al., 2020; Michaud et al., 2021), or muscle-induced stress development in skeletal bodies (Moody et al., 2009; Phillips et al., 2015; Favier et al., 2021; Favier et al., 2021); (4) in clinical applications in predicting the outcome of surgical procedures (Delp, S. L. et al., 1990; Giat, Yohanan et al., 1994; Tigue et al., 2022) or optimizing rehabilitation (Sartori et al., 2012; Hassani et al., 2014; Ai et al., 2016; Peng et al., 2016), or for the design and control of prosthetics (Manal et al., 2002; Eilenberg et al., 2010; Farina et al., 2017; Niu et al., 2020; Farina et al., 2021); or (5) sports-related applications, like optimizing performances (Edman et al., 1978; Pandy et al., 1990; Anderson & Pandy, 1999) or predicting the effects of muscle fatigue on performance (Giat, Y. et al., 1993; Liu, J. Z. et al., 2002; Callahan et al., 2016; Potvin & Fuglevand, 2017; Penasso & Thaller, 2018; Sharma et al., Jan 01, 2009).

Hill-type models are therefore flexible and can fulfil different objectives, with a suitable compromise between model complexity and accuracy. To choose the optimal Hill-type variant, one must have a clear understanding of the content of the literature in Hill-type modelling. Yet, the field of Hill-type modelling is currently extremely dense, with over a thousand models proposed in the past 50 years, and hard-to-explore since the last available narrative reviews date back 20 years or more and the more recent studies investigating the existing modelling approaches and assessing the gaps in the literature are not exhaustive. While this situation drastically limits knowledge transmission and complicates for everyone the time-consuming identification of the 'right' Hill-type model in the literature, it also slows down the pace of innovation, despite important remaining limitations, as discussed in this study, as it is difficult to build upon an ill-defined state-of-the-art. This situation also promotes detrimental tendencies, such as ill-referencing, inter-study inconsistency in terminologies, definitions and notations, and overlooking most recent contributions. As advised in the 90s (Epstein, 1998), contemporary literature and systematic reviews of the literature must be available to organize and clarify the contents and state-of-the-art of the field, as recently done in skeletal muscle continuum modelling (Dao & Tho, 2018), multiscale neuromuscular modelling (Röhrle, Oliver, Yavuz et al., 2019), cervical spine MSK modelling (Alizadeh et al., 2020), and lower limb force modelling during gait (Trinler et al., 2018).

In this respect, this study provides the first systematic review of the field of Hill-type muscle-tendon modelling. Its contents and state-of-the-art are assessed with two scoring schemes, a completeness assessment, and a modelling evaluation, applied to a set of 55 eligible studies, that were extracted from a systematic search for published Hill-type models. The eligible studies were chosen to be representative of all the modelling approaches taken to describe 23 properties underlying the muscle-force generation process. The completeness assessment identifies which muscle properties are described in an eligible model, while the modelling assessment evaluates the level of validation and

reusability of the model and attention given to its modelling strategy and calibration. The results of the scoring schemes are used to discuss the current trends and gold standards in Hill-type modelling, challenge them, investigate the state-of-the art, identify the current gaps and lines of improvement, and open the discussion on the necessity of global recommendations to promote model reusability and knowledge transmission against the current scarcity of open-source models and lack of consensus on good practices. This study is supported by extensive supplementary material and can be used as a convenient time-saving tool to navigate through the literature, as any published model can be retrieved by combining the modelling approaches proposed in the eligible studies, and to develop novel Hill-type models answering current limitations.

Methods

This systematic review was performed following the PRISMA guidelines (Moher et al., 2009), the commented checklist of which is provided in SM2.

Terminology, definitions, and acronyms

The definition of a Hill-type model has been continuously refined and extended since Hill's preliminary Nobel prize-winning works (Hill, 1922; Hill, 1938; Barclay & Curtin, 2022), as detailed in SM1. A Hill-type model refers today, consistently with the terminology proposed in milestone reviews in the field (Zajac, 1989; Winters, Jack M., 1990; Epstein, 1998), to any rheological arrangement of an active force generator (FG), which builds the active muscle force, and in-series and in-parallel MT passive elements, which passively transmit force through the stretch-resisting dynamics of their constitutive material. In the literature, the behaviour of these active and passive rheological elements is governed by mathematical expressions that describe up to 23 phenomenological passive or active MT properties, which are displayed along with their acronyms in Table 1 and Figure 1.

In this review, the contractile element (CE) and the neuromechanical element (NE) interact to define the FG (Figure 1). The CE lumps any of the 10 CE-related contractile properties (Table 1) that describe the multiscale mechanical events that occur during the active contraction dynamics of the FG. The NE groups the events involved in the neuromechanical interface between the central nervous system and the muscle machinery; it accounts for the excitation, activation, and motor unit (MU) recruitment dynamics of the neuromuscular system, that define the neural control to the CE.

For future purposes, a 'baseline' Hill-type model (Figure 2) refers to any rheological arrangement of one passive element, one NE and one CE, the behaviour of which is respectively described by one passive property, one CE-related property, and one NE-related property. In the following, a Hill-type model is termed 'innovative' if it provided a methodological contribution to the field at the time of its publication, and more precisely a novel modelling approach for at least one of the 23 properties reported in Figure 1, that could not be retrieved from a previously published paper identified from the systematic search. For conciseness and simplicity in this review, proposing novel rheological arrangements, new mathematical descriptions for previously published methodological approaches, and new ways of identifying the parameter values scaling those mathematical expressions were chosen not to be criteria to identify a model as 'innovative'.

If not stated otherwise, this review only refers to 'generic' models (Zajac, 1989), that are normalized by the subject-muscle-specific slack length of the Series Elastic Element (SEE), the optimal length of the CE and the muscle maximum isometric force. For simplicity and conciseness, muscle pennation is disregarded in this review, despite limitations for highly-pennated muscles (Zajac, 1989; Scott & Winter, 1991; Carbone et al., 2016). Consistently with the literature, the passive elements and their respective constitutive property are described with the same acronym in the following.

Table 1: Hill-type models are described with 9 possible rheological elements and 23 possible phenomenological properties. This table provides for these elements and properties brief descriptions and the acronyms that are used in this review. ADL, ADV, FLA, FVL and FVA refer to a nonlinear dependency of the model activation dynamics (AD) and Force-Length (FL) and Force-Velocity (FV) relationships to the model active (A), length (L) and velocity (V) states.

Rheological element	Properties	Acronym	Description and corresponding physiological events and mechanisms
NE (Neuromechanical Element)	Excitation dynamics	ED	Electro-chemical dynamics of the neural drive from the spinal pre-synaptic input to the depolarization of the nerve axons (neural ED – nerve action potentials (APs)) and of the muscle fibre sarcoplasm and T-tubules (muscle ED – muscle APs)
	Motor unit recruitment dynamics	MURD	Dynamics of the motor unit recruitment
	Activation dynamics	AD	Dynamics of the excitation-contraction coupling properties from the release of calcium ions Ca^{2+} in the sarcoplasm to the transient myosin-actin cross-bridge attachment mechanism
	Calcium-dependent activation dynamics	ADC	Explicit inclusion of a sub-model of the transient dynamics of calcium concentration in the model of AD
	Length-dependent activation dynamics	ADL	Inclusion of the nonlinear dependency of the AD to the length of the CE, that affects calcium transients and enhances the probability of troponin-calcium binding and of cross-bridge formation (Blinks et al., 1978; Rassier et al., 1999)
	Velocity-dependent activation dynamics	ADV	Inclusion of the nonlinear dependency of the AD upon the velocity of the CE
CE (Contractile Element)	Force-length relationship	FL	Phenomenological instantaneous isometric relationship at maximal muscle activation between the CE length and the CE force, consistently with the sliding filament theory and the average myosin-actin overlap in the sarcomeres
	Activation-dependent force-length relationship	FLA	Inclusion of the nonlinear activation-dependency of the FL relationship accounting for the phenomenologically decreasing optimal CE lengths with higher activation levels
	Concentric Force-velocity relationship	FVC	Instantaneous relationship at maximal activation and optimal CE length between the concentric / eccentric contraction velocity and force of the CE. It relates to the varying probability of cross-bridge attachments between sliding sarcomere filaments and to the titin activation dynamics
	Eccentric Force-velocity relationship	FVE	
	Length-dependent force-velocity relationship	FVL	Nonlinear length-dependency of the FV relationship, involving lower maximum shortening velocity at decreasing lengths below optimal CE length

	Activation dependent force-velocity relationship	FVA	Nonlinear activation-dependency of the FV relationship, involving an increased value of maximum shortening velocity and decreased curvature of the relationship with higher levels of activation
	Force depression	FD	Decrease in the isometric muscle force after active shortening compared to purely isometric conditions, potentially related to titin activation dynamics
	Residual force enhancement	RFE	Increase in the isometric muscle force after active lengthening compared to purely isometric conditions, potentially related to titin activation dynamics
	Other time-history dependent mechanisms	OTHD	Sag: a short-term force decrease specific to fast fibres Yield: a slow force decrease related to an increasing rate of cross-bridge detachment during isotonic contractions reducing the number of cross-bridges (Brown et al., 1999) Short-range stiffness: a short-term force increase/ decrease at the beginning of a lengthening/ shortening task, attributed to deformation of attached muscle cross-bridges
	Fatigue	Fat	A decline in the ability of a muscle to generate sustained force over time
PEE	Parallel passive stress-strain relationship	PEE	Instantaneous force-length relationship of parallel tissue structures passively resisting muscle stretch
PEE2	2nd parallel passive stress-strain relationship	PEE2	Instantaneous force-length relationship at short lengths accounting for the deformation of the sarcomeres building a repulsive passive force
PDE	Parallel passive force-velocity relationship	PDE	Instantaneous force-velocity relationship accounting for the viscoelastic properties of the parallel passive structures
M	Muscle inertia	M	Muscle mass, impacting the inertial dynamics of the MT complex
SEE	Series passive stress-strain relationship	SEE	Stress-strain relationship accounting for the passive resistance to stretch of in-series tendinous and / or muscular tissues; usually models the behaviour of the tendon, in which case it is often referred as T in the literature
SEE2	2nd series passive stress-strain relationship	SEE2	Stress-strain relationship accounting for the passive resistance to stretch of in-series muscular and musculotendinous tissues; usually models the stiffness of the cross-bridges, of the titin in active conditions, and of the aponeurosis
SDE	Series passive force-velocity relationship	SDE	Instantaneous force-velocity relationship accounting for the viscoelastic properties of the in-series passive structures

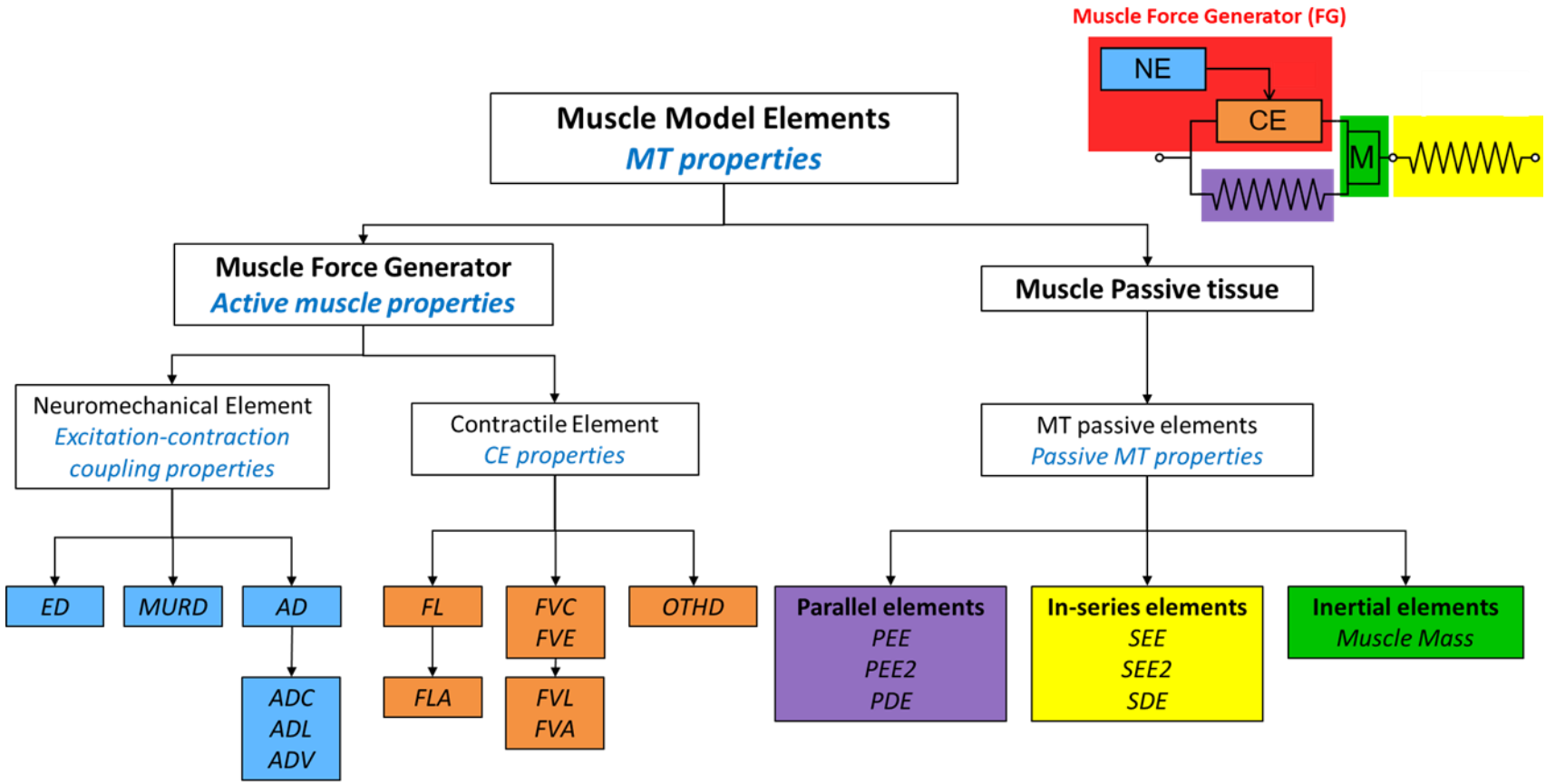

Figure 1: Hill-type models typically include MT passive elements and a muscle Force Generator (FG). In the FG, the Neuromechanical Element describes the muscle's excitation-contraction coupling properties (light-blue boxes) and drives the muscle Contractile Element, described by the contractile properties (orange boxes) and responsible for force generation. Some properties are nonlinearly dependent to the level of activation (FLA, FVA), length (ADL, FVL) and contraction velocity (ADV) of the FG. Besides inertial elements (green box), Hill-type models include passive elements in-parallel (purple box) and in-series (yellow box) with the FG. The acronyms for the 9 rheological elements and the 23 muscle properties are defined in Table 1.

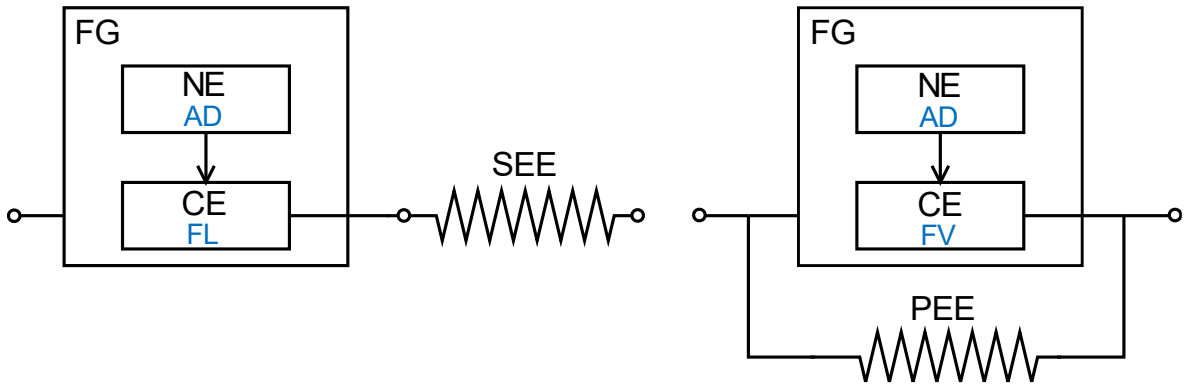

Figure 2: Example of two 'baseline' Hill-type models. They include one passive element (Left: SEE and Right: PEE), and an FG that involves a NE, described here by one AD property, and a CE, described here by one FL (Left) or FV (Right) relationship. The acronyms are defined in Table 1.

Systematic search for eligible studies

The research studies published between 1938 and 25/09/2022 that involved a Hill-type model were systematically searched for on four computational databases: PubMed, Web of Science, MedLine via Web of Science and EMBase via Ovid. Specific keyterms, reported in SM3, were searched for in the titles and abstracts of the research studies. The keyterms were grouped into four concepts (C1 to C4) listed in Table 2 with OR Boolean operators. The four groups of keyterms were then joined into a unique search string of the form 'C1 AND C2 AND C3 NOT C4'. Details on the search strategy are provided in SM2 and SM3. The results of the systematic search were stored by year of publication in the reference manager Mendeley.

The final set of 'eligible' studies retained for scoring assessment was identified according to six eligibility criteria (EC1 to EC6) listed in Table 2, aiming for milestone studies that provide detailed descriptions of 'complete' Hill-type models representative of the genesis and the state-of-the-art in Hill-type modelling. After removing duplicates, the studies that did not meet EC1 to EC5 were chronologically removed based on title screening, abstract screening, and if necessary, screening of the core text of the paper. The filtering was then repeated with the reference lists of the papers that passed EC1 to EC5, to identify further potentially eligible studies that were missed by the systematic search. The final set of studies that met EC1 to EC5 were chronologically compared for application of EC6. To identify the 'innovative' studies, inheritance diagrams were built for the AD, FL, FV, PEE and SEE properties to map over the past fifty years the chronological chain of references between studies. The inheritance diagrams distinguish the parent studies that proposed novel modelling approaches to the field from the child studies that took inspiration from or replicated the parent ones.

Table 2: Definition of the four keyterm concepts C1-C4 for the systematic search. Definition of the eligibility criteria EC1-EC6.

C1	The Hill-type MT model
C2	The muscle, the tendon
C3	The model, the actuator, the simulation
C4	The smooth muscle, the cardiac muscles
EC1	The studies are Journal articles in English
EC2	Only skeletal muscles are considered
EC3	The muscle model is of the Hill-type
EC4	An explicit description of the properties of at least a 'baseline' Hill-type model is provided
EC5	The dynamics of the model rely on length- and force- dependent state variables
EC6	The model is 'innovative'

Scoring assessments

Completeness assessment

Each eligible model was assessed for 'completeness' by scoring 1 for each of the 23 properties (Figure 1) that was included in the Hill-type model, yielding a 'completeness' score out of 23, with a minimum of 3 according to EC4. According to Table 1, the modelling of the NE, CE and passive elements can respectively score 6, 10 and 7, yielding a balanced significance between these three types of elements. The completeness score enables an inter-study assessment of the level of complexity and the relative modelling strengths and weaknesses of the eligible models for mimicking the true muscle neuromechanical interface, mechanical events, and passive dynamics. The average score across eligible studies for each property was also calculated to identify the most common practices and gaps in Hill-type modelling.

Modelling assessment

Four methodological practices (I-IV) considered by the reviewers to be crucial for a suitable transmission of incremental knowledge in the field of Hill-type modelling were reviewed in a 'modelling assessment' of the eligible studies. With the 10 questions (Q1 to Q10) listed in Table 3, it was evaluated the strategy taken by the eligible studies for (I) model validation, (II) promoting model reusability, (III) detailing the modelling choices, strategy, and limitations, and (IV) model calibration. Q1 to Q10 were scored 0, 1 or 2, which indicate no, incomplete and satisfying methodological practice respectively, and yield a 'modelling score' out of 20. To avoid bias and subjectivity, a detailed scoring grid was built for each question before the studies were assessed and is provided in SM4.

Table 3: The 10 questions constituting the modelling assessment. The eligible studies can score 0, 1 or 2 to these questions according to a detailed scoring scheme provided in SM3.

Practices	Question number	Questions
(I) Model Validation	1	Is the accuracy of the predictions obtained with the Hill-type model assessed against ad hoc experimental data?
	2	Is the model validated against reliable muscle-specific experimental quantities?
	3	Is the accuracy of the model evaluated with quantitative mathematical metrics?
(II) Model reusability	4	Is enough information provided in the study to fully reimplement the computational model and reproduce the results published in the study?
	5	Is the model optimized for numerical stability and computational speed?
(III) Modelling choices and strategy	6	Are the taken simplifications in modelling the rheological actuator clearly stated?
	7	Are the modelling choices of the rheological model clearly stated and / or justified with respect to the objectives of the study?
	8	Is there a discussion about the strengths and limitations of the normalized Hill-type model?
(IV) Model calibration	9	Are the mathematical expressions describing the properties of the Hill-type model scaled with experimental data consistent with the scope of the study?
	10	Is the Hill-type model scaled or normalized with species-patient- or muscle-specific scaling parameters?

Global score

For each eligible paper, the completeness and modelling scores were normalized by 23 and 20 respectively and averaged to yield a final global score in percentage. The global score measures the global degree of completeness, validation and reusability of an eligible model and the level of attention given to its modelling strategy and calibration. The global score is not an indicator of the overall quality of the eligible studies, considering that some of them were not modelling studies, with focus and contributions beyond the scope of the scoring assessments.

Results

Systematic search for eligible studies

The systematic search returned 55 eligible studies, listed in Table 4, that meet EC1 to EC6 (Table 2). As displayed in the flowchart in Figure 3 (see SM5 for additional details), the three databases returned 2492 journal articles in English without duplicates, among which 125 were identified by the reviewers to meet EC2 to EC5. After screening the reference lists, 163 studies were carefully screened in several iterations to apply EC6, using the inheritance diagrams stored in supplementary material as support. Fifty-five eligible models met EC6 for the reasons listed in SM6, while the 98 excluded studies were either replicates or a combination of the 55 eligible models. As displayed in Figure 3, 61 non-eligible studies were retained and briefly analysed in SM7 because 32 of them proposed models, assessed for completeness in SM8, that were innovative (EC6) but did not meet EC4, while the others brought significant contributions to the field of Hill-type modelling, including narrative reviews, sensitivity analyses, or comparisons between published models. The 55 eligible (Table 4) and 32 non-eligible (SM7) models that meet EC6 are considered to be representative of all the modelling approaches proposed to date in the field of Hill-type modelling for the properties listed in Table 1.

As displayed in Table 4, 32 of the 55 eligible studies aimed to develop the field of Hill-type modelling by proposing innovative muscle models and investigating the sensitivity of model predictions to parameter values, challenging some modelling assumptions, or investigating the strengths and limitations of Hill-type models to predict some physiological mechanisms. Eight eligible studies developed new methods to use Hill-type models in neuromusculoskeletal simulations. Fourteen eligible studies used Hill-type models to investigate physiological mechanisms including some material stress-strain dynamics, joint mechanisms related to muscle activity, posture and motion control in response to perturbations or the muscle redundancy problem. For clarity, the studies are referred to 'First Author Year of publication' in the figures of this review. Also, the two eligible complementary studies (Kim et al., 2015; Kim & Kim, 2018) were grouped together in this review.

Table 4: List of the 55 eligible models and the main aim of their related study

Topic of the study	References
Advancing the field of Hill-type modelling	(Bahler, 1968; Hatze, 1977; Hatze, 1978; Giat, Y. et al., 1993; Durfee & Palmer, 1994; Van Zandwijk et al., 1996; Nussbaum & Chaffin, 1998; Curtin et al., 1998; Shue & Crago, 1998; Brown et al., 1999; Cheng et al., 2000; Ettema & Meijer, 2000; Lloyd & Besier, 2003; Thelen, 2003; Günther et al., 2007; Mavritsaki et al., 2007; Song et al., 2008; Menegaldo & Oliveira, 2009; Tsianos et al., 2011; Maceri et al., 2012; Blümel et al., 2012; Mörl et al., 2012; Callahan et al., 2013; Millard et al., 2013; Lee et al., 2013; Elias et al., 2014; Kim et al., 2015; Hamouda et al., 2016; Dick et al., 2017; Kim & Kim, 2018; Siebert et al., 2018; Ross, Nigam et al., 2018; Rockenfeller, R. et al., 2020; Hussein et al., 2022)
Developing methods for including Hill-type models in neuromusculoskeletal simulations	(Wyss & Pollak, 1984; Pierrynowski & Morrison, 1985; Otten, 1987; Winters, J. M., 1995; Dorgan & O'Malley, 1997; Kistemaker et al., 2006; Proctor & Holmes, 2010; Wang et al., 2012)
Investigating physiological mechanisms using Hill-type models	(Bobbert & van Ingen Schenau, Gerrit Jan, 1990; van Soest & Bobbert, 1993; Happee, 1994; Caldwell, 1995; DeWoody et al., 2001; Gallucci & Challis, 2002; McLean et al., 2003; Stelzer & Von Stryk, 2006; Gömmel et al., 2007; Moody et al., 2009; Rengifo et al., 2010; John et al., 2013; Marcucci et al., 2017; Warner et al., 2020)

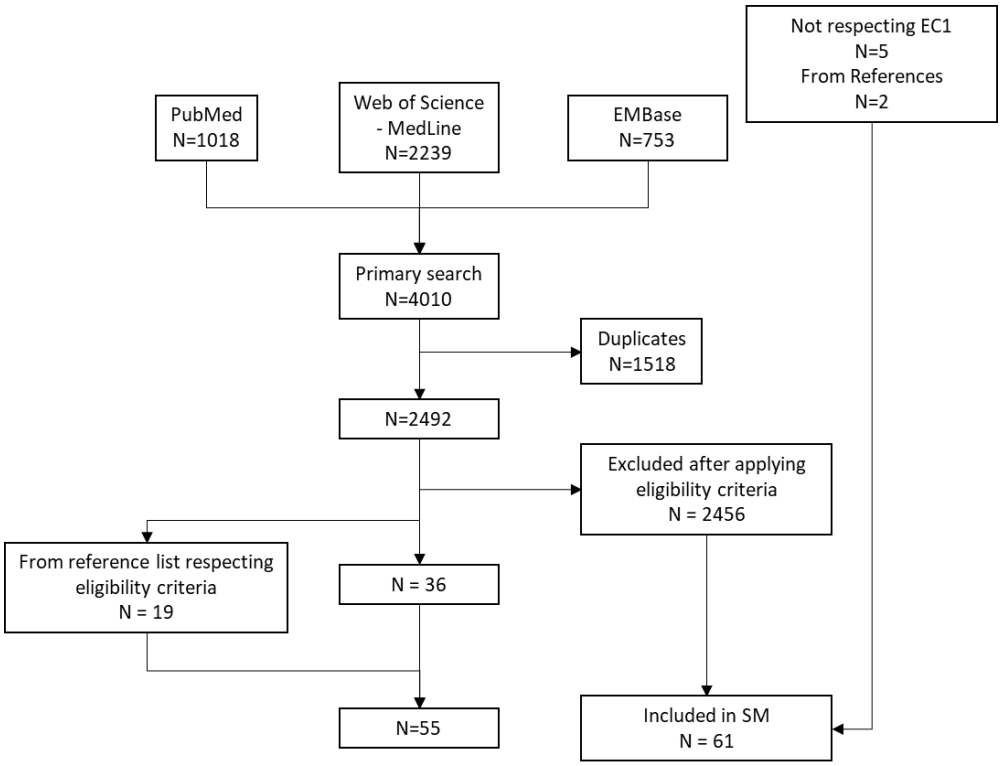

Figure 3: Flowchart of study inclusion according to EC1 to EC6. 36 eligible studies were obtained from the systematic search and 18 from the reference lists of the studies respecting EC1 to EC5. 61 non eligible studies were listed in SM7 and investigated in SM8 for their important contribution to the field of Hill-type modelling. See SM5 for a more detailed version of this diagram.

Completeness assessment

General results

The per-study results of the completeness assessment are displayed in Figure 4 (additional details in SM8). The 55 eligible models scored in the range [3-16] out of 23 possible MT properties (mean: 8, standard deviation: 2.6) and showed no correlation between model completeness and publication year. As shown in Figure 5A, most of the models included between seven and nine MT properties, seven models included five or fewer properties, consistently with the model description by Zajac (1989), and five models included at least 12 properties (Winters, J. M., 1995; Dorgan & O'Malley, 1997; Cheng et al., 2000; Song et al., 2008; Tsianos et al., 2011), that is more than half of the identified muscle properties reported in Table 1. The specific properties included in each of the 55 eligible studies can be identified in the bar graph in SM8. The rheological arrangements of the eligible models are displayed in SM9.

Modelling trends

The frequency graph in Figure 5B shows that the six properties AD, FL, FVC, FVE, PEE and SEE are widely considered key in Hill-type modelling as they respectively appear in 98%, 96%, 98%, 83%, 76% and 85% of the eligible studies. These most popular properties have been described and extended in the past 50 years with various modelling approaches and mathematical descriptions, the time-evolution of which is detailed in SM10 with inheritance diagrams and a summary of the mathematical equations proposed in the eligible studies.

The dynamics of the NE are most commonly lumped with a phenomenological model of AD consisting of a transient first-order ordinary differential equation (ODE) inspired from (Winters, Jack M. & Stark,

1988; Zajac, 1989; He et al., 1991; Winters, J. M., 1995) in 30 of the 55 eligible studies, or with a steady-state nonlinear transfer function (7/55), mostly sigmoidal with advanced physiological interpretability (Rockenfeller & Günther, 2017a), while several other eligible studies (17/55) describe the calcium dynamics (Hatze, 1977; Hatze, 1978; Otten, 1987) in an ADC approach. A quarter of the eligible models (15/55) drove the muscle AD with an excitatory drive derived from a model of ED, including for example feedback controllers (3/55), first-order phenomenological ODEs (8/55) or comprehensive compartmental Hodgkin-Huxley-like models of the motoneuron discharging mechanisms (Proctor & Holmes, 2010; Kim & Kim, 2018). A quarter of the eligible models (13/55) considered the dynamics of MU recruitment (MURD) with, for example, detailed phenomenological models (Hatze, 1978; Dorgan & O'Malley, 1997; Callahan et al., 2013), simpler models relying on recruitment thresholds (4/55), or different recruitment characteristics for slow and fast representative units identified from EMG wavelet analysis (Lee et al., 2013; Dick et al., 2017).

The dynamics of the CE are dominantly modelled (50/55) with a length-dependent FL relationship, that linearly scaled by the active state, and is typically described with quadratic (11/55) (Woittiez et al., 1984) and gaussian (16/55) (Hatze, 1977) mathematical descriptions according to SM10 (see (Rockenfeller & Günther, 2017b) for a review). One study (Hamouda et al., 2016) tackled the issue of the non-physiological instability of the descending limb of the FL relationship. Most eligible studies (39/55) modelled the FVC relationship with Hill's two-parameter or normalized hyperbola (see SM10), the 20% force overestimation of which near static conditions is tackled with a double-hyperbolic shape (Curtin et al., 1998). Around a third (21/55) of the eligible studies modelled the FVE relationship with a two-parameter hyperbolic curve inspired from (Mashima et al., 1972; FitzHugh, 1977), while less than a quarter (12/55) used an inverted hyperbola respecting a C2 continuity between concentric and eccentric FV branches.

The muscle passive properties are typically modelled with a PEE and/or a SEE, described as nonlinear passive springs, the stress-strain relationships of which are mostly defined with quadratic (Bobbert & van Ingen Schenau, Gerrit Jan, 1990; van Soest & Bobbert, 1993), exponential (Hatze, 1977), and piecewise linear-exponential (Otten, 1987; Giat, Y. et al., 1993) expressions (see SM10). Approximately half of the eligible studies (25/55) used a linear PDE to model the slight viscoelasticity of the muscle's inner passive structures, or to prevent numerical singularities when inverting the FV relationship.

Less commonly modelled properties

As shown in Figure 5B, between 10% and 30% of the eligible studies enrich the aforementioned modelling approaches by considering a PEE2 (10/55), describing the short-length repulsive force due to sarcomere deformation, muscle mass (13/55), accounting for muscle-specific inertial characteristics and preventing numerical instabilities (Cheng et al., 2000; Song et al., 2008), or the nonlinear state-dependency of the ADL (12/55), FVL (15/55) and FVA (15/55) relationships. The eight remaining properties listed in Table 1 (ADV, FLA, FD, RFE, OTHD, Fat, SEE2 and SDE) are rarely modelled and appear in less than 10% of the eligible studies. As seen in Figure 5C, most of the least commonly modelled properties have not been considered in the eligible models in the past ten years and were mostly developed in the 1990s and 2000s.

Model parameters

Most eligible studies maintained low model complexity, as half used between 5 and 14 parameters to define their normalized properties, a third used 15 to 24 parameters, and 5 studies used more than 35 parameters up to around 60. As supported by SM8, on average two parameters were used to define one property, with higher ratios for the studies modelling the MURD (Hatze, 1978) or comprehensive descriptions of the NE (Proctor & Holmes, 2010; Kim & Kim, 2018).

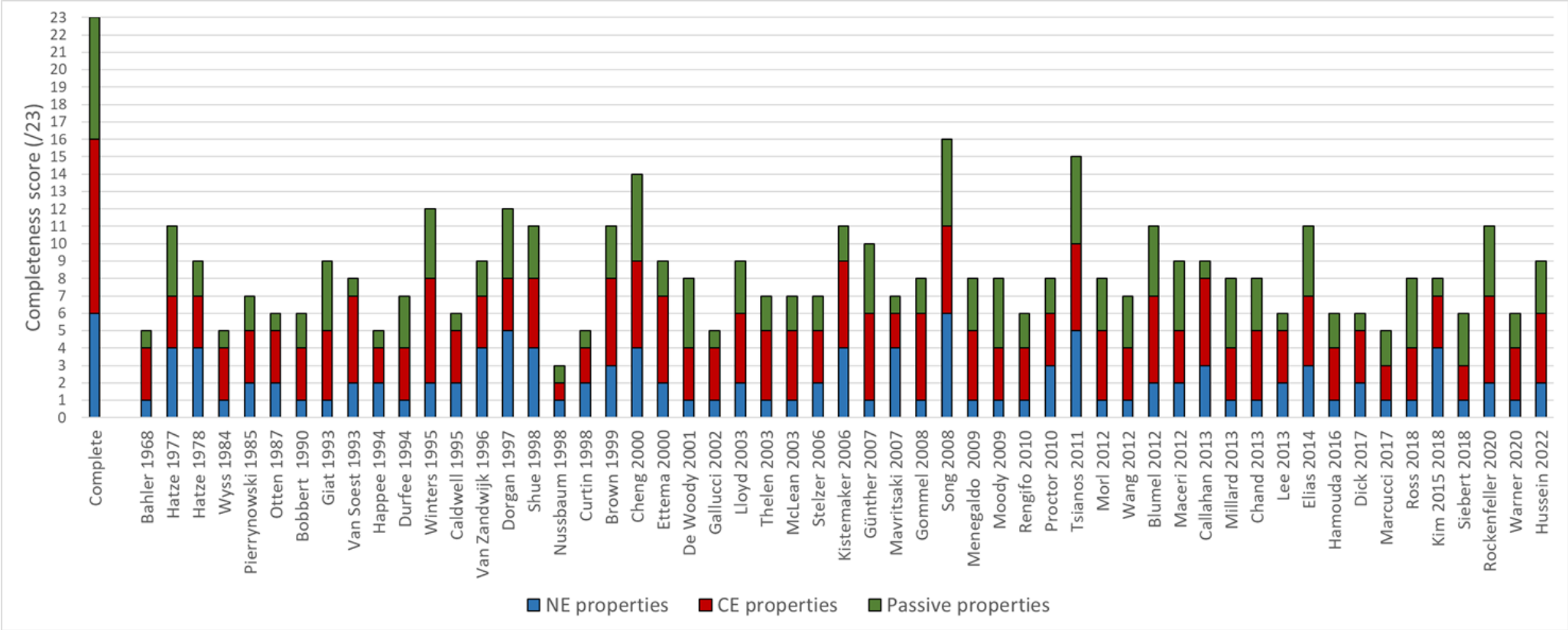

Figure 4: Results of the completeness assessment for the 55 eligible studies. A 'complete' bar representative of a theoretical complete model is provided for comparison. Blue: the 6 properties of the NE. Red: the 10 properties of the CE. Green: the 7 properties of the passive elements. The 55 studies are chronologically ordered. A more detailed version of this graph is provided in SM8.

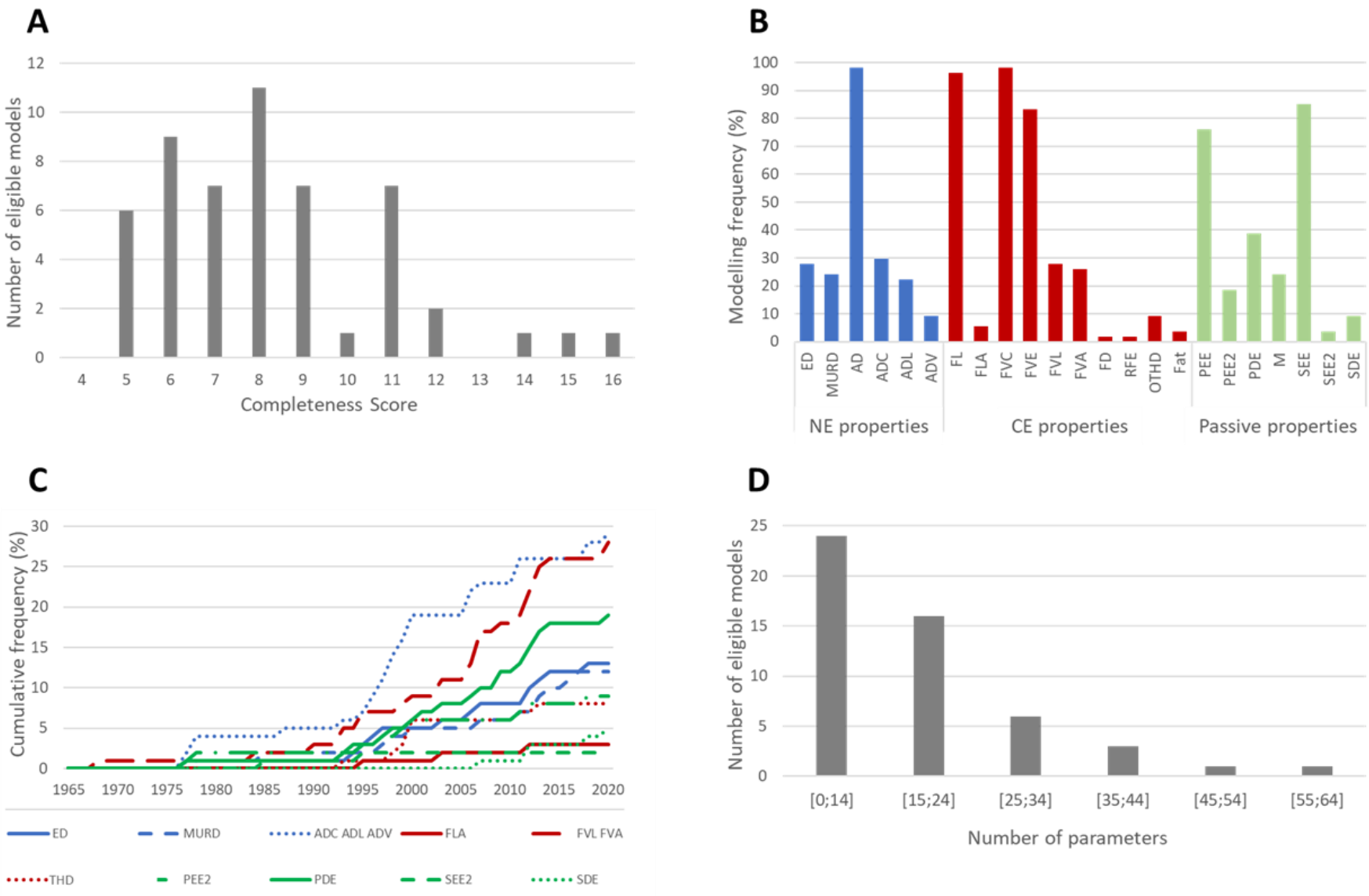

Figure 5: Results of the Completeness Assessment of the 55 eligible studies. (A) Frequency distribution of the eligible models according to their completeness score (out of 23). (B) Modelling frequency of each of the 23 properties among the eligible studies, where the modelling occurrence of each property is normalized to a percentage. (C) Time-accumulation of the eligible models that considered the 12 least commonly modelled properties. For clarity, some properties are grouped together: ADC-ADL-ADV, FVL-FVA, and FD-RFE-OTHD-Fat under 'THD'. (D) Frequency distribution of the eligible models according to their number of parameters

Modelling assessment

Global results

Figure 6A shows that the eligible studies scored in the range [4-18] out of 20 (mean: 11, standard deviation: 3.5), 22 studies scored less than 10/20, and 9 studies scored above 15/20. The per-study results of the modelling assessment are displayed in Figure 7 (additional details in SM11) and show no correlation between modelling score and publication year. As shown in Figure 6B, the four categories (validation, reusability, modelling choices and strategy, and calibration) detailed in Table 3 globally received the same level of attention with average scores of 1.0, 1.0, 1.2 and 1.2 respectively, while the eligible studies scored an average in [0.8-1.2] for most questions, except Q3 and Q5 for model optimization and model reusability which scored below 0.75/2. SM12 reports for Q1 to Q10 the most popular modelling approaches proposed in the eligible studies.

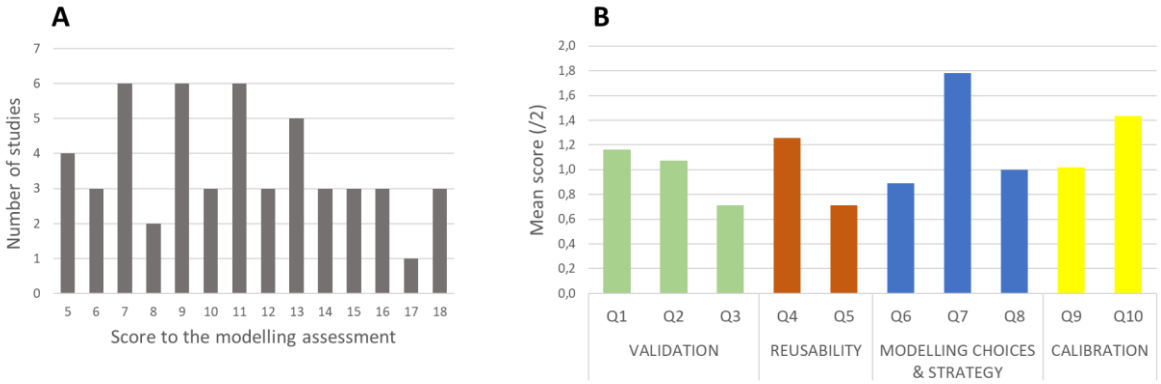

Figure 6: (A) Distribution of the 55 eligible studies according to their total score in modelling assessment (out of 20). (B) Mean scores among the 55 eligible studies for the 10 questions of the modelling assessment. The yielded mean scores are out of 2.

Model validation (Q1 to Q3)

Less than half of the eligible studies (25/55) validated the model predictions against ad hoc experimental animal data, mostly mammalian muscle force (10/55) or human (15/55) quantities such as joint torque (12/55). A quarter (15/55) of the studies proposed validations against results from available experimental datasets, the protocol of which were reproduced in simulations, and the remaining eligible studies (15/55) either proposed no model validation or qualitative validations against other results from the literature. Less than a third (17/55) of the eligible studies used mathematical or statistical metrics for the analysis and interpretation of the model predictions, while the remaining studies (38/55) only proposed qualitative and visual assessments of their analysis. Consequently, approximately a third of the eligible studies proposed sufficient validation for a complete evaluation of the performance of their model.

Model reusability (Q4 and Q5)

Approximately two thirds (36/55) of the eligible studies did not provide enough information to make possible a re-implementation of their Hill-type models and a reproduction of the published results, missing some reference or some description for the chosen rheological arrangement, the mathematical equations describing the modelled properties, and/or the parameter values scaling these properties. Out of the 19 remaining eligible studies, which presented models that could theoretically be re-implemented, only five provided full access to the actual implementation of their computational model (Cheng et al., 2000; Mavritsaki et al., 2007; Song et al., 2008; Millard et al., 2013;

Kim & Kim, 2018), while open-source versions for two more (Thelen, 2003; John et al., 2013) were then made available as the result of other studies. Most of the eligible models (37/55) were not optimized for stability and computational speed, while eight imposed C1 or C2 continuity for all modelled properties, and twelve avoided singularities in the inverted FV relationship (see SM12 for additional details). Consequently, most of the eligible models cannot be readily reused in other studies.

Modelling choices and strategy (Q6 to Q8)

More than half of the studies (33/55) commented on some modelling simplifications and assumptions regarding the muscle physiology and geometry, while less than a third (16/55) discussed the multiscale modelling approach. Around three quarters of the eligible studies (43/55) justified their modelling choices with references and in accordance with the aim of the study, although most of them (40/55) did not discuss and compare the strengths and weaknesses of the modelling approach in relation to other studies in the literature. Consequently, most of the eligible studies do not draw conclusions on the future works necessary to improve their model.

Model calibration

Around a third (21/55) of the eligible studies made at least one of the model properties subject-muscle-specific by tuning its parameters either with parameter calibration minimizing a cost function between simulated and experimental quantities, or with ad hoc experimental measurements. Half of the eligible studies (28/55) used the aforementioned methods to scale the normalized Hill-type model with subject-specific values for the slack length of the Series Elastic Element (SEE), the optimal length of the CE and the muscle maximum isometric force. Consequently, most of the eligible models are generic.

Global assessment

Figure 8 provides the global score for the 55 eligible studies. A high score globally suggests that an eligible model describes numerous muscle properties, is carefully described, calibrated, and validated, and is easily reusable. However, the global score is not an indicator of the overall quality of the eligible studies. The eligible studies scored in the range [26%; 67%] (mean: 46%, standard deviation: 12%). Ten eligible studies scored below 33%, 25 in the range [33%; 50%], and nine above 60% (Hatze, 1978; Shue & Crago, 1998; Cheng et al., 2000; Günther et al., 2007; Song et al., 2008; Tsianos et al., 2011; Blümel et al., 2012; Millard et al., 2013; Kim et al., 2015; Kim & Kim, 2018).

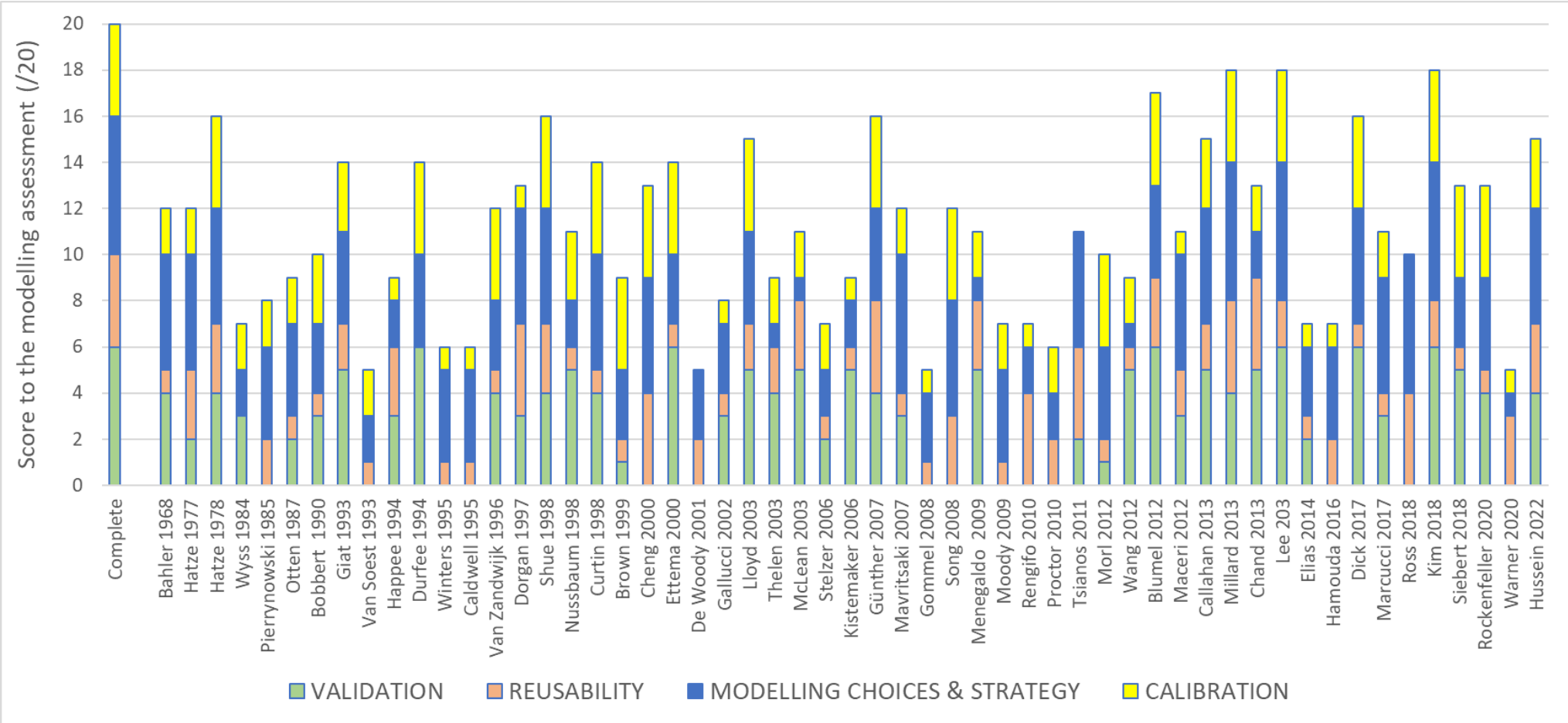

Figure 7: Results of the modelling assessment for the 55 eligible studies. A 'complete' bar representative of a model scoring 2 to the 10 questions is provided for comparison. Green: model validation. Red: Model reusability. Blue: Modelling choices and strategy. Yellow: model calibration. A more detailed version of this graph is provided in SM11.

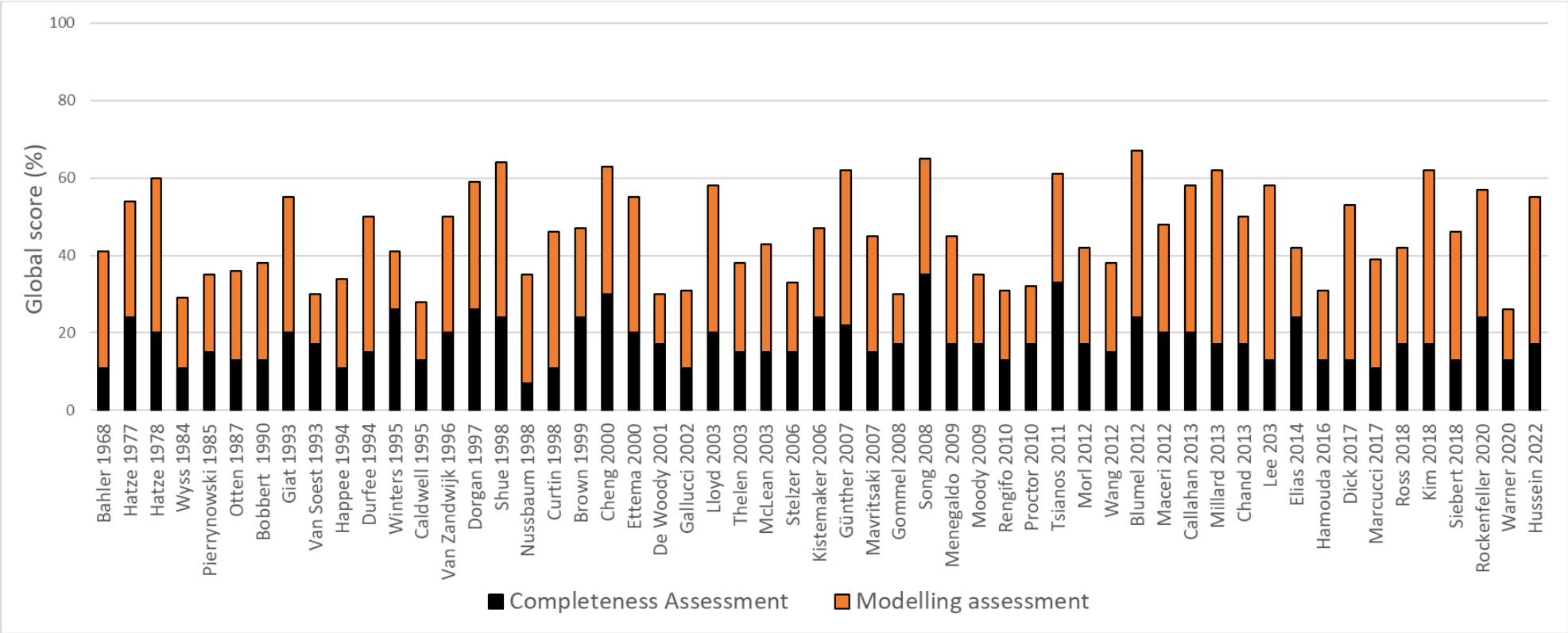

Figure 8: Global scores for the 55 eligible studies. Completeness (black) and modelling (orange) assessments were given the same weights to derive the global score.

Discussion

Summary and main objectives

This systematic review clarifies the dense and hard-to-explore field of Hill-type modelling, for which recent reviews are lacking, and provides a tool for researchers to identify the current trends in Hill-type modelling and to assess the state-of-the-art and current gaps in property modelling and methodological practices. To meet these objectives, 55 eligible studies (Table 4), which were extracted from the systematic search (Figure 3) according to six eligibility criteria (EC1 to EC6, Table 2) that impose a minimum level of model complexity (Figure 2) and innovation (SM6), were investigated according to two scoring schemes. In the following, the results of the completeness and modelling assessments (Figure 4 to Figure 8) are used to (1) define the main trends and gold standards in Hill-type modelling, (2) challenge these gold standards with advanced modelling methods, (3) clarify the state-of-the-art by investigating properties non-commonly modelled in the field, (4) discuss the importance of model validation, and (5) open the discussion on the necessity of more regular reviews and global recommendations in the field of Hill-type modelling, with an emphasis on model reusability for optimal transmission of knowledge.

How to use this study?

Besides clarifying the contents and current challenges of the field of Hill-type modelling for non-specialists, this study provides, with Figure 4, Figure 7 and Figure 8 (more detailed versions in SM8 and SM11), a simple tool to researchers to guide their choice towards the best available published Hill-type models to address the aims of their study with respect to model completeness, validation, reusability, or calibration, and modelling choices and strategy. Using as support the list of published reviews, sensitivity analyses and comparative studies in SM7, modelers can also take inspiration from the following discussion and the extensive supplementary material provided in this review on the current trends and state-of-the-art in modelling approaches and methodological practices to develop new models to answer the current gaps in the field. The set of 87 (55 eligible (Table 4) and 32 non-eligible (SM7) Hill-type models reported in this study is representative of all the modelling approaches proposed in published Hill-type structures for modelling the properties listed in Table 1 and displayed in Figure 1. Detailed reviews of the rheological structures proposed in the field, and of the main modelling approaches for properties ADC, AD, FVC, FVE, FVL, FVA, FL, FLA, PEE and SEE are proposed respectively in SM9, and in SM10, with lists of mathematical equations and inheritance diagrams. The properties modelled by the 87 studies can be identified with the bar graphs resulting from the completeness assessment in SM8, while the model complexity can be inferred from the number of model parameters in Figure 5D and SM8. The reader interested in open-source solutions is referred to SM13, the GitHub repository https://github.com/modenaxe/awesome-biomechanics, and to the open-source implementation of the models used in the OpenSim platform (Delp et al., 2007; Seth et al., 2018; Dembia et al., 2020).

Main trends and gold standards in Hill-type modelling

According to the conclusions drawn in the Results Section from the completeness and modelling assessments, to Figure 5B, Figure 6B for Q6-8 and to SM12, Hill-type models in the literature are most commonly described with a Voigt-Kelvin structure that includes a NE, a CE, a PEE and a SEE (see examples in SM9) to model the 'classic' AD, FL, FVC, FVE, PEE, SEE properties in a multiscale approach where a representative muscle fibre represents the whole muscle. Typically, a single phenomenological ODE produces a time-history-dependent active state $a(t)$ that describes the lump

activity of the muscle's neuromuscular interface, and linearly scales the instantaneous length-dependent and velocity-dependent forces $f_{FL}(l^{FG})$ and $f_{FV}(v^{FG})$ determined by the independent CE's FL and FV properties, to define the total FG force f^{FG} as $f^{FG}(t, l^{FG}, v^{FG}) = a(t) \cdot f_{FL}(l^{FG}) \cdot f_{FV}(v^{FG})$. The FG, in-parallel with the PEE, is in equilibrium with the SEE, which passively transmits the active force as $f^{SEE} = f^{FG} + f^{PEE}$. These equations define a common baseline for most of the Hill-type models in the literature and are typically rearranged to isolate and solve for unknown state variables, such as the FG length l^{FG} or force F^{FG}. The most common mathematical descriptions for the AD, FL, FV, PEE and SEE properties are reported in SM10.

Challenging the gold standards in Hill-type modelling

The aforementioned gold standards in Hill-type modelling, most of which were proposed between 1938 and 1976 (see SM1 for details), can be challenged and the main trends in defining and modelling the multiscale approach, the FL and FV properties, the active state, the interplay between the NE and the CE and the in-series passive elements can be extended.

Multiscale approach

Hill-type models are flexible enough to describe, with a single actuator and adequate multiscale simplifications, the structure and dynamics of either individual sarcomeres, fibres, MUs or, most commonly, whole muscle-tendon systems. Despite successfully reducing the cost and complexity of Hill-type muscle modelling, multiscale approaches come with important assumptions. When a whole muscle is described as one of its 'representative' unidirectional fibre or MU, it implies that all muscle fibres or MUs have homogeneous 'average' material properties and dynamics, and are in parallel, coplanar, of the same length spanning across the whole muscle length, making the same pennation angle with the tendon and simultaneously excited with the same neural control and electromechanical delay with an homogeneous repartition of activated fibres across the muscle, and work independently without lateral force transmission. Multiscale sarcomere-to-muscle approaches further imply that the muscle's sarcomeres all have the same length and neuromechanical characteristics and work independently from their in-parallel neighbours. These multiscale simplifications may contradict experimental data ((Blemker & Delp, 2005; Blemker et al., 2007), for example), preventing modelling of some muscle properties, such as MURD, and affecting the physiological accuracy of the muscle description with limitations in reconciliating microscopic and macroscopic scales and mechanisms (Winters, Taylor M. et al., 2011; Wisdom et al., 2015; Hou, 2018; Günther et al., 2018), with subsequent potential downgrades in prediction accuracy (Huijing & Slawnych, 2000).

Yet, only a few eligible studies (see SM11 and Figure 6 Q6-7), including the 9 modelling single fibres or MUs with a Hill-type model, explicitly evoke the multiscale approach and its implications on Hill-type modelling. This lack of clarity feeds and is strengthened by a lack of consensus between studies in the notation defining the muscle quantities, with 22 different notations observed in the eligible studies for the length of the contractile unit ($L, L_M, L_{CE}, L_m, L_f, L_{fibers}, L^M, L^m, L^F, l, l_{CE}, l_{CC}, l_m, l_f, l_{ce}, l^M, l^{CE}, X_m, x, x_{eye}, x_{CE}, \lambda$), and often the same notation (l or l_m) for different quantities (muscle and muscle-tendon length). Overlooking the multiscale conditions, the eligible studies often use experimental data to fit the Hill-type properties at a scale inconsistent with the modelled physiology. This is an important limitation, as the FL relationship is for example known to be piecewise linear at the sarcomere scale but to be smoother with larger plateau (Hatze, 1980) and more slowly decreasing descending limb beyond optimal fibre length at larger scales (Herzog, Walter et al., 2015), a multiscale difference sometimes debated (Winters, Taylor M. et al., 2011; Moo et al., 2020). Also, the curvature of the FV relationship decreases with higher scales (compare (Ranatunga, 1982; McDonald et al., 1994; Roots et al., 2007) for works on rat skinned fibres, bundles of fibres, and whole muscles), while the Young's

modulus in the exponential stress-strain relationship of the PEE nonlinearly increases from the fibre to the muscle scale (Ward et al., 2020), with dominant contributions to the total passive force of the titin structures and of the extracellular matrix at the fibre and muscle scales respectively (Prado et al., 2005; Ward et al., 2020; Wheatley, 2020). Consequently, the multiscale Hill-type modelling must be correctly applied and commented to maintain credible descriptions of the muscle physiology and dynamics.

FL, FV and FVL properties

Current gold standards in FL and FV modelling can be advanced. The non-physiological instability in the classic description of the descending limb of the FL relationship can be corrected with a time-history-dependent approach accounting for the initial length at activation onset (Hamouda et al., 2016), or with a two-mode Hill-type model (Akazawa, 2019; Akazawa, 2020). Recent advances on our understanding of the active FL curve can be considered in future models, such as the usually overlooked important role of the length-dependent interfilament spacing and electrostatic interaction on the ascending arm of the FL relationship (Rockenfeller et al., 2022). To avoid an overestimation of instantaneous force at low shortening velocities, the FVC relationship should be modelled as double-hyperbolic (Edman et al., 1978; Edman, 1988; Curtin et al., 1998; Edman, 2005; Alcazar et al., 2019), while the standard FVE modelling reaching higher-than-F_0^M forces during eccentric contractions is experimentally challenged (Sutarno & McGill, 1995). As modelled in only a few eligible studies (Figure 5B), the FVC property nonlinearly varies with instantaneous muscle length (Askew & Marsh, 1998) as the maximum shortening velocity decreases with shorter sub-optimal muscle lengths (Abbott & Wilkie, 1953; Gordon et al., 1966; Bahler, 1968), despite a lack of consensus (Edman, 1979; Edman, 1988), and the curvature of the FVC relationship (defined by the a_f parameter in SM10) decreases with shorter sub-optimal muscle lengths (Granzier et al., 1989) and increases for longer over-optimal lengths (Edman, 1988), suggesting an increased probability of cross-bridge attachment during filament sliding when the inter-filamentary spacing is reduced, which can be debated to be redundant with the properties described by the FL relationship.

Definition of the muscle active state

The active state of a CE is commonly defined as the intracellular concentration of calcium ions (Thelen, 2003) or the proportion of available troponin receptors bound to calcium ions (Ebashi & Endo, 1968). These definitions prevent extending the phenomenological description of the NE behaviour to subsequent important transient events that are typically not reflected in the instantaneous CE properties, such as the calcium-troponin binding dynamics or the probabilistic cycling mechanism of cross-bridge formation between detached, weak bound and force-generating states (Shorten et al., 2007; Tamura et al., 2008; Zot & Hasbun, 2016), that are typically overlooked in Hill-type modelling. We suggest defining the active state of a CE as the normalized instantaneous ratio of formed cross-bridges in the force-generating state in a population of myosin heads, irrespective of the degree of filamentary overlap, relative inter-filamentary sliding speed and other external mechanical mechanisms, which should be modelled in the contraction dynamics of the CE. This definition is not paradoxical with any influence fibre length or velocity can have on the mechanisms involved in the overall AD discussed below. To the authors' knowledge, only three analytic (Wexler et al., 1997; Ding et al., 2000; Neidhard-Doll et al., 2004) and five Hill-type models (Otten, 1987; Van Ruijven & Weijs, 1990; Rassier et al., 1999; Wilson et al., 2006; Mavritsaki et al., 2007) have proposed phenomenological time-dependent ODEs to explicitly account for the transient mechanisms occurring between the events of calcium ion release and force generation, which are typically lumped with a steady-state pCa-force sigmoidal relationship (Hatze, 1977; Lloyd & Besier, 2003).

Interplay between the NE and the CE – FLA, ADL, FVA, ADV properties

The real muscle mechanisms rely on an interplay between the CE's and NE's activation, length, and velocity states, which is commonly overlooked in Hill-type models as shown in Figure 5B and SM8. Modelling the behaviour of the NE to be independent from the state of the CE and linearly scaling with the active state the FL and FV relationships, which are typically obtained from experimental observations at maximal muscle activity, are important limitations which partly explain the poor performance of Hill-type models in submaximal activation tasks (Perreault et al., 2003). As performed in some of the eligible studies (Figure 5B), this interplay is considered with ADL, ADV, FLA and FVA approaches, which are potentially redundant, and where the FG properties are nonlinearly related to the active state a, length l^{FG} and velocity v^{FG} as described in SM10.

The FL relationship is empirically observed (Rack & Westbury, 1969; Stephenson & Wendt, 1984; Guimaraes et al., 1994; Huijing, 1996; Balnave & Allen, 1996; Rockenfeller & Günther, 2018; Goislard de Monsabert et al., 2020) and mechanistically explained (Rockenfeller et al., 2022) to distort for submaximal contractions towards peak forces occurring at longer CE lengths. It is explained, at the CE level, by changes in the force transmission pathways between the multiscale layer of the muscle (Huijing, 1999) to minimize the muscle internal work and optimize force production (Holt & Azizi, 2014). The FLA property is phenomenologically captured in three eligible models (Winters, J. M., 1995; Lloyd & Besier, 2003; Blümel et al., 2012) with an activation-dependency of the CE optimal length $l_0^{FG}(a)$, which improves the accuracy of the model predictions (Sun et al., 2018). However, it is believed that the FLA approach phenomenologically encapsulates in these studies some ADL properties at the NE level (Rassier et al., 1999), that are responsible for the length-dependencies of the experimental frequency-force (Rack & Westbury, 1969; Brown et al., 1999), EMG-force (Goislard de Monsabert et al., 2020) and pCA-force (Stephenson & Williams, 1982) relationships. It is proven that the calcium transients are length-dependent (Blinks et al., 1978; Baylor, S. M. et al., 1983; Close & Lännergren, 1984; Konishi et al., 1991) as the muscle geometry affects the dynamics of calcium release from the sarcoplasmic reticulum and calcium diffusion in the sarcoplasm. The reaction rate for calcium-troponin (CaTn) unbinding decrease with increase sarcomere length (Matsuo et al., 2010). Furthermore, lengths above l_0^{FG} increase the sensitivity of cross-bridge formation to calcium ions (Endo, 1973; Moisescu & Thieleczek, 1979; Stephenson & Williams, 1982; Stephenson & Wendt, 1984), and the probability of cross-bridge formation by geometrically reducing the intrafilamentary spacing between myosin and actin filaments (Godt & Maughan, 1981). The latter phenomenon may be redundantly modelled with the FVL approach described previously.

The modelling of a nonlinear a-dependency of the FVC relationship (FVCA) proposed in 14 eligible studies is justified by the important decrease in maximum shortening velocity with decreasing activation observed in human joint torques (Chow & Darling, 1999; Camilleri & Hull, 2005), cat dissected muscles (Petrofsky & Phillips, 1981) and in rabbit skinned fibres (Moss, 1986) and explained by an increase in inactive inertia (Ross & Wakeling, 2016). Yet, this phenomenon could also be modelled as an ADV property in the NE because of both a lower ratio of fast-contracting MUs at low activation, and an increase in the number of cross-bridges bearing tensile force against shortening dynamics, as cross-bridge detachment rates slow with lower levels of sarcomeric calcium concentration. While denied (Camilleri & Hull, 2005) or neglected in a suitable manner (Winters, J. M., 1995), three eligible studies (Winters, J. M., 1995; Günther et al., 2007; Blümel et al., 2012) consider another FVCA property, where the curvature of the FVC relationship decreases at higher activation (Petrofsky & Phillips, 1981; Bayer et al., 2017), which is potentially explained by the lower ratio of slow versus fast recruited MUs, which exhibit different FV contractile properties. Five eligible studies (Brown et al., 1999; Cheng et al., 2000; Song et al., 2008; Tsianos et al., 2011) proposed an ADV property to

model the yielding phenomenon, which relies on the same physiological mechanisms as short-range stiffness (Malamud et al., 1996) during eccentric contractions. Upon stretch deformation, cross-bridges provide rapid tensile stiffness (Campbell & Lakie, 1998; Getz et al., 1998) before forcibly detaching leading to the force drop related to yielding (Sutarno & McGill, 1995), the effects being emphasized in slow-type fibres (Malamud et al., 1996; Brown et al., 1999) in fast eccentric contractions (Nichols, 1984; Malamud et al., 1996), where the rates of cross-bridge detachment (Joyce et al., 1969) and attachment are respectively higher and slower. Therefore, the SRS dynamics should be modelled as a passive property (De Groote et al., 2017), while yielding is both a passive and a time-history dependent FVA property, for the decrease of weak-bound and force-generating cross-bridges respectively due to mechanical stretches. Although SRS and yielding should not be modelled in the NE according to the definition of AD previously proposed, they influence the time-course of the muscle ED and MURD (Cordo & Rymer, 1982; Sutarno & McGill, 1995).

In-series elastic elements

Tendon slack length and stiffness have a key influence on model predictions, according to the sensitivity studies reported in SM7. The tendon behaviour is commonly modelled with an SEE in-series with the FG (see SM9 for rheological structures) and simple nonlinear stress-strain relationships (see equations in SM10). Besides complicated multiscale tendon models (Maceri et al., 2012), advanced phenomenological models of the tendon behaviour that would for example account for its hysteresis (Herzog, Walter, 2019) have however not yet been proposed in the literature of Hill-type modelling. Most eligible models describe the additional passive activity of the muscle aponeurosis and other sub-scale passive structures with a SEE2, although they should be considered in-parallel with the FG and included in the PEE in first approximation (Herzog, Walter, 2019). In sarcomere-scale Hill-type structures, a SEE2 can however encapsulate the passive titin and cross-bridge elasticities, which are in-series with the force-generating cross-bridges, although they are mechanically not in-series with the macroscopic tendon due to the in-parallel arrangement of laterally-connected myofibrils and fibres, contradicting some previous sarcomere-to-muscle multiscale modelling approaches (Pierrynowski & Morrison, 1985; Zajac, 1989; Pandy et al., 1990). To avoid such inaccurate simplifications in sarcomere-to-muscle multiscale approaches, it is advised to neglect the SEE2 dynamics when the elasticity elastic energy storage is predominantly taken by a long and/or compliant free tendon (Zajac, 1989). The increment in tendon velocity-dependent stiffness arising from the SDE viscoelasticity can be likewise neglected for slow-to-medium contraction speeds (van Ingen Schenau, G J et al., 1988; Meijer et al., 1998; Mörl et al., 2012).

Current gaps in Hill-type modelling and lines of improvement

According to the results of the completeness assessment in Figure 4 and Figure 5A, the eligible studies globally score relatively low (mean and median of 8/23) and do not extend the baseline approach (Figure 2) much beyond the gold standards discussed previously. Individually, they however tackle numerous gaps in Hill-type modelling and open the field to new lines of improvement, some of which were discussed in the previous section.

Modelling the neuromechanical interface

Most eligible studies limit the modelling of muscle's excitation-contraction coupling properties to a 'black box' 1st-order ODE and/or a steady-state sigmoid transformation (see SM10 for examples) to transform the excitation state into the active state of the FG. Such models of AD are hardly relatable to actual physiological mechanisms and are therefore difficult to interpret, calibrate, validate, and advance (Hussein et al., 2022). This is a major limitation when numerous highly nonlinear mechanisms actually define the subject-muscle-task neuromechanical dynamics of the MU pool and the neural

drive to muscle, and are proved to have a dramatic influence on force generation (Heckman & Enoka, 2012; Farina & Negro, 2015). To tackle this limitation, more complex modelling approaches must be proposed to describe the discrete NE dynamics, from the spinal synaptic influx to the definition of the active state previously proposed.

In this respect, some eligible studies (17/55) explicitly model the time-course of the calcium transients in the sarcoplasm (see SM10 for equations). In describing actual physiological mechanisms, this ADC approach enables a confident modelling of the length-dependency of the AD dynamics, discussed previously, and a direct validation against experimental (Hollingworth, S. et al., 1996; Baylor, S. M. & Hollingworth, 2003) or simulation (Baylor, S. M. & Hollingworth, 1998; Holash & MacIntosh, 2019) studies evaluating calcium transients and pCa-force relationships. When modelling ADC, it is worth noting the preferable choice of the mag-2-fura indicator in experimental studies, as well as the strong dependency of the calcium transients to animal species and temperature (Hirota et al., 1989; Raju et al., 1989; Konishi et al., 1991; Delbono & Stefani, 1993; Delbono et al., 1995; Zhao et al., 1996; Capote et al., 2005; Hollingworth, Stephen et al., 2008; Baylor, Stephen M. & Hollingworth, 2011; Hollingworth, Stephen et al., 2012). While some comprehensive models of calcium transients (Shorten et al., 2007; Heidlauf & Röhrle, 2014; Pizarro & Olivera, 2020) can also be included in Hill-type models, additional AD dynamics such as the CaTn transients have been proposed in a recent MN-driven Hill-type model (Caillet et al., 2022).

As suggested in Figure 5B, because of the limitations related to the fibre-to-muscle multiscale approach, most eligible studies disregard the dynamics of MURD and Henneman's size principle (Henneman, 1957; Henneman, 1981; Henneman, 1985). The MU recruitment, discharge and mechanical properties are inter-related, MU-specific, and continuously distributed across the MU pool from small low- to large high-force and -threshold MUs, as quantitatively reviewed (Caillet et al., 2022), and the relative importance of MURD and discharge frequency in the determination of the neural drive to muscle is task-dependent (Heckman & Enoka, 2012). In most multiscale eligible studies, it is unclear whether the complete MU pool is assumed to be recruited at all times and the excitation state is an indicator of the overall MN discharge frequency, or if the excitation state, typically obtained from processed EMG signals in this case, is a lump representation of the MU pool recruitment and discharge dynamics. To avoid confusion, some studies proposed a phenomenological model of MURD in a single multiscale NE (Hatze, 1978; Hatze, 1980; Legreneur et al., 1996; Riener et al., 1996; Dorgan & O'Malley, 1997; Riener & Fuhr, 1998; Song et al., 2008; Tsianos et al., 2011; Callahan et al., 2013). Recent studies also proposed an explicit description of the MURD with a complete reconstruction of the MU pool in muscle models built as a collection of MUs described analytically (Raikova et al., 2018), with Hill-Huxley-type structures (Carriou et al., 2019) or with Hill-type actuators (Caillet et al., 2022). The MURD are described with the model from Fuglevand et al. (1993) in the first two studies, while other approaches could be considered (Heckman & Binder, 1991; Liu, J. Z. et al., 2002; Dideriksen et al., 2010; Dideriksen et al., 2011; Dideriksen et al., 2012; Potvin & Fuglevand, 2017; Petersen & Rostalski, 2019). MU pool reconstruction makes it easier to describe the distribution of the MU neuromechanical properties in the muscle, which can also be lumped in two FGs for slow-type and fast-type populations (Wakeling, James et al., 2012; Lee et al., 2013; Dick et al., 2017).

MU pool reconstruction and detailed models of the MURD motivate an advanced modelling of the ED, i.e. of the electrical-chemical mechanisms underlying the time-course of the MU-specific neural message from the spinal synaptic influx to the depolarization of the t-tubules. In the literature, analytical, phenomenological or Hodgkin-Huxley-like approaches are proposed to model the discharge trains of action potentials that drive MU-scale Hill-type models (Hatze, 1977; Hatze, 1978; Happee, 1994; Legreneur et al., 1996; Van Zandwijk et al., 1996; Mavritsaki et al., 2007; Proctor & Holmes, 2010;

Maceri et al., 2012; Kim et al., 2015; Kim & Kim, 2018) and permit realistic reconstruction of the MU force as a summation of individual twitches, as opposed to muscle-scale approaches that receive continuous neural controls, such as EMG-driven models. The modelling of the robust process of neuron-fibre synaptic transmission that always elicits post-synaptic action potentials (Bigland-Ritchie et al., 1982; Wood & Slater, 2001; Kovyazina et al., 2010) can be neglected.

It is worth noting that both the modelling of the ED and MURD can be by-passed if MN spike trains and their intrinsic discharge and recruitment dynamics are experimentally obtained, e.g. by decomposing high-density surface EMG (HDEMG) signals (Del Vecchio et al., 2020) or intramuscular recordings (Muceli et al., 2022) and extended to the recruitment and discharge behaviour of the complete MU pool with physiologically realistic methods (Caillet et al., 2022). This approach is technically challenging but it is preferable over merging these MN-specific quantities into a unique neural control to muscle-scale models (Sartori et al., 2017; Thompson et al., 2018; Kapelner et al., 2020).

Titin-induced time-history-dependent mechanisms

The classic steady-state instantaneous CE properties should be extended to describe the muscle time-history dependent transient properties, as performed in a few eligible models (Figure 5B), to avoid potential high prediction errors (Winters, Jack M., 1990) and describe certain behaviours like balance control against perturbations (Seiberl et al., 2013; De Groote et al., 2017). While comprehensive models of muscle fatigue exist (Shorten et al., 2007), the proposed methods for modelling FD and RFE in Hill-type models are phenomenological and not related to the physiological mechanisms responsible for these time-history dependent properties. RD and RFE are explained by the various dynamics of titin (Herzog, W. et al., 2016; Tahir et al., 2020), rather than the nonuniformity of sarcomere lengths (Herzog, Walter et al., 2015). Titin can shorten with calcium-mediated binding (Herzog, W. et al., 2010; Herzog, Walter et al., 2015) or winding (Hessel et al., 2017) motions and increase its stiffness upon activation (Bagni et al., 2002; Bagni et al., 2004; Powers et al., 2014; Rassier et al., 2015), which besides stabilizes the aforementioned descending limb of the instantaneous FL relationship (Schappacher-Tilp, 2018). With an unfolding-folding behaviour at activation (Brynnel et al., 2018), titin can also provide power strokes to the force-generating cross-bridges and accelerate muscle shortening (Rivas-Pardo et al., 2016; Eckels et al., 2019). Consistent with the previously discussed ADL properties, titin promotes cross-bridge-attachment by passively pre-stretching non-active sarcomeres (Fusi et al., 2016; Piazzesi et al., 2018). Already included in Huxley-type (Rode et al., 2009; Schappacher-Tilp et al., 2015) and continuum (Heidlauf et al., 2017) models, the titin activity could be modelled in a hybrid CE-PEE property that alternates between active (Li et al., 2018) and passive (Brynnel et al., 2018; Ward et al., 2020) states, and is in-series or in-parallel with the cross-bridges upon calcium activation (Herzog, Walter, 2019).

Inertial effects

Although it typically increases the numerical cost of the model by involving 2nd-order ODEs, considering muscle mass in Hill-type models can increase numerical stability (Cheng et al., 2000) and reduce the muscle maximum shortening velocity and mechanical work (Ross & Wakeling, 2016; Ross et al., 2020). A mass element is necessary to investigate the contraction-related effects of muscle mass flow (Guo et al., 2020), on which depends the MSK centre of mass location, and wobbling masses (Gruber et al., 1998) on the reduction of impact forces (Liu, W. & Nigg, 2000; Gittoes et al., 2006), joint contact forces and torques (Gruber et al., 1998; Pain & Challis, 2006), or bone internal stresses (Moody et al., 2009).

Choice of parameters

The behaviour of the NE, CE and passive elements is highly dependent on the parameter values that describe the properties displayed in Figure 1 and discussed previously. These parameter values, which are typically obtained from fitting experimental data with parametrized mathematical relationships, vary with multiscale considerations as discussed, and are mostly also species-, muscle-, temperature-, and subject-specific. For example, the a_f parameter describing the curvature of the FVC relationship increases from fibre- to muscle-scale as discussed, and between slow-type and fast-type fibres (Bottinelli et al., 1996; Bottinelli et al., 1999; Widrick et al., 2002), while the parameter defining the half-time of relaxation of the calcium transients (ADC) drastically decreases with increasing temperatures (Hollingworth, S. et al., 1996), between slow and fast fibres (Baylor, Stephen M. & Hollingworth, 2012) and between mammalian (Baylor, S. M. & Hollingworth, 2003) and amphibian (Hatze, 1977) species. Potentially because of limitations in knowledge transmission in the field of Hill-type modelling, discussed later in this section, it was observed that most eligible studies overlooked the importance of these numerical values (Figure 6B Q9), which were not provided in most publications. Several eligible studies proposed CE and passive properties described with parameters experimentally obtained from different species and typically copied from milestone but dated Hill-type modelling studies (Hatze, 1977; Otten, 1987; Winters, J. M., 1995). More recent experimental data are usually not exploited as dated frog data (Gordon et al., 1966) is commonly used over more recent human data (Gollapudi & Lin, 2009) to describe human muscles.

According to sensitivity studies listed in SM7 (Scovil & Ronsky, 2006; Redl et al., 2007; Xiao & Higginson, 2010; De Groote et al., 2010; Ackland et al., 2012; Carbone et al., 2016; Bujalski et al., 2018), the predictions of muscle forces in MSK simulations are most sensitive to three MT parameters: the tendon slack length, the optimal length of the CE and the muscle isometric force. It is worth noting that these observations were made with mostly 'baseline' models, and additional sensitivity studies on 'more complete' models are required to generalize these conclusions. While the parameters describing the muscle properties can remain generic, these three scaling parameters must be tuned to be subject-muscle-specific (Zajac, 1989). As referenced in SM12, some eligible studies (Hatze, 1978; Bobbert & van Ingen Schenau, Gerrit Jan, 1990; Lloyd & Besier, 2003; John et al., 2013; Kearney et al., 2021) proposed calibration methods, although various configurations of parameter values can explain similar muscle dynamics (Bujalski et al., 2018), depending on the role of the muscle in the MSK task (Carbone et al., 2016; Bujalski et al., 2018; Kian et al., 2021). Other eligible studies experimentally measured these properties in animal (Giat, Y. et al., 1993; van Soest & Bobbert, 1993; Günther et al., 2007) or human (Dick et al., 2017) ad hoc experiments, or used available experimental datasets (Brown et al., 1999; Callahan et al., 2013). Some also scaled the MT parameters using subject-specific anthropometric measurements and generic literature data (Cheng et al., 2000; Menegaldo & Oliveira, 2009; Wang et al., 2012; Dick et al., 2017). In this approach, recent datasets obtained from large populations of young adults and recent experimental techniques should be preferred for estimating the FG optimal length (Ward et al., 2009) and the muscle maximum isometric force (Handsfield et al., 2014), as performed previously (Rajagopal et al., 2016), to smaller dated datasets (Wickiewicz et al., 1983; Delp, 1990) obtained from specimens of advanced age that present important age-related muscle atrophy and smaller PCSAs (Young et al., 1984; Klein et al., 2001; Thelen, 2003; Hasson & Caldwell, 2011). Finally, close to half of the eligible studies used generic data from the literature to determine these parameters.

Principles of model validation

The performance of a muscle Hill-type model can be evaluated by comparing its predictions against experimental quantities obtained in situ or from complete experimental datasets made available in the literature (Perreault et al., 2003; Wakeling, James M. et al., 2021). The gold standard quantity for model validation is the time-course of individual fibre or muscle forces, which can be obtained or derived from dissected muscles of anesthetized animals as in some of the eligible studies, from non-invasive ultrasound measurements of fascicle or tendon length in humans (Lichtwark et al., 2007; Dick et al., 2017; Monte et al., 2020; Zhang et al., 2021; Zhang et al., 2022), or from specific protocols that minimize muscle co-activation during joint torque measurements (Hatze, 1981). Since the latter methods are relatively complex, most models are validated by comparing experimental and predicted joint torques, also often used for model calibration for the same activity, joint angles, and neural EMG-like signals, as discussed in the Results Section and detailed in SM12, despite limitations in validation accuracy as simulated and experimental quantities accumulate errors independent from muscle contraction mechanisms. In all cases, different experimental datasets must be used for model calibration and validation. Finally, the validation of model performance should be quantified with mathematical metrics (see SM12 for details related to the eligible studies) to prevent qualitative assessments and bias and improve readability. These important considerations were overlooked by many eligible studies (Figure 6B, Figure 7).

Once validated, a model may be implemented in other studies providing its performance is objectively considered in light of the modelling choices taken and the physiological plausibility of the calibrated parameter values. Most eligible studies overlooked such practices, as reported by the modelling assessment (Figure 6B Q3 and 6 to 8). Model reusability is also promoted when published results can be reproduced, which is possible when the model can be fully reimplemented, either with an open-source implementation of the model, or from a detailed description in the text of the modelled properties, rheological arrangement of the elements, parameter numerical values and methods for solving the muscle dynamics, most of which the eligible studies failed to provide (SM12 and Figure 6B Q4 and 5).

Limitations of the study

This systematic review, despite following the PRISMA recommendations (see SM2), comes with a few limitations related to the custom design of the eligibility criteria and scoring schemes.

By constraining the eligible models to the six EC in Table 2, milestone studies specialized in research areas interfacing with the modelling of MT properties in Hill-type models were overlooked, including for example advances in parameter estimation (Modenese et al., 2016; Falisse et al., 2016), volumetric muscle definitions (Woittiez et al., 1984; Modenese & Kohout, 2020), the optimization of computational runnability (Van Den Bogert, Antonie J et al., 2011; De Groote et al., 2016), MSK modelling (Delp, S. L. et al., 2007; Rajagopal et al., 2016) and in-vivo neural inputs for motor control (Sartori et al., 2017; Thompson et al., 2018; Kapelner et al., 2020). Besides disregarding other types of muscle models (EC3), such as Huxley-type (Zahalak, 1981; Lemaire et al., 2016; Carriou et al., 2019) and continuum (Röhrle et al., 2012; Röhrle, Oliver et al., 2019; Gfrerer & Simeon, 2021) approaches, some key 'innovative' Hill-type models that met EC6 but did not include a NE (EC4) were also not considered for global scoring in this study; to complement the extensive results presented in this study for the 55 eligible studies, those 32 additional studies are reported in SM7 and assessed for completeness in SM8. Besides, although it provides a window on the state-of-the-art in Hill-type modelling, the application of EC6 biases the results towards concluding that the field of Hill-type modelling is populated with rather more complete Hill-type models (Figure 4, mean: 8/23) than the

majority of models proposed in the literature, which are actually closer to baseline models (Figure 2) and would score 5/23 or less.

Besides the 23 properties considered in this study, some important neuromuscular properties, such as the titin dynamics, were not considered for completeness assessment, as they were never described in Hill-type models. Also, it is important to reiterate that the completeness assessment provides information about the complexity of a model and its capacity to describe specific muscle mechanisms but does not provide any indication on the quality of the modelling approach. Likewise, the outcomes of the modelling assessment do not provide any indication on the accuracy of the eligible model predictions. The choice of model complexity and number of parameters, a key topic in Hill-type modelling (Audu & Davy, 1985), could have been considered in this scoring scheme, beyond the results in Figure 5D. Although care was taken to achieve a balanced scoring approach, as discussed in the Methods Section for both the scoring schemes, some modelling and methodological approaches may be under-represented, like the choice of rheological structure or the use of the multiscale simplifications that only account for 2.5% of the global score each (Figure 8). Finally, if the 55 eligible models are representative enough of the field of Hill-type modelling to describe its state-of-the-art, they may not be representative of the methodological approaches globally taken in the literature about model validation, reusability, modelling choices and strategy and calibration (Table 4). This reduced window may weaken the impact of some conclusions drawn from the Modelling Assessment in this Discussion Section, considering for example that some non-eligible studies would have reached high modelling scores (Siebert et al., 2008; Hasson & Caldwell, 2011).

Required recommendations in the field of Hill-type modelling

As shown in the chronological graph in Figure 5C, the state-of-the-art in Hill-type modelling seems to have plateaued since the 80s-90s when substantial modelling innovations occurred. It is notably observed that following the turn of the century modelling advances have focussed on describing discrete muscle properties and never build upon other contemporary innovations, as they keep relying on the 50-year-old gold standards, rather than challenging their important limitations, discussed previously. This tendency is typical of a dense field, for which the most recent narrative reviews (listed in SM7) date back 20 years or more, and where the transmission of knowledge is therefore limited. To permit innovation and incremental breakthroughs, Epstein (1998) stresses the importance of regular literature reviews to periodically clarify and summarize the field, update on its state-of-the-art and avoid the emergence of detrimental inclinations that further aggravate the situation. One of them is the increasing inconsistency observed between the eligible studies in terminology and notations referring to, for example, the multiscale FG length as optimal length, normalized length, maximum isometric force, tendon slack length, maximum force in eccentric contractions, but also in the definition of isometric contraction as constant muscle or muscle-tendon lengths. Another detrimental tendency is the chain of references between Hill-type studies breaking over time; in such case, inheritance diagrams (SM10) are necessary to trace the current modelling techniques back to their source studies. This unclear literature also pushes researchers towards reusing and not adapting the milestone studies from the 80s-90s with more recent available experimental data, as discussed previously. In this context, the lack of systematic good practices stressed by the modelling assessment (Figure 6B) further hinders the transmission of knowledge and the reusability of published models, as it is difficult to build upon a model that is not carefully validated and described, and for which no open-source implementation is available. In these conditions, researchers seem rather to opt for open-source ready-to-use models (Schutte et al., 1993; Thelen, 2003; Millard et al., 2013; John et al., 2013), as 20% of the studies obtained from the systematic search and respecting EC1 to EC3 since 2006 used

the muscle models embedded in the simulation platform OpenSim (Delp, S. L. et al., 2007; Seth et al., 2018). While these models are shown to make good and fairly accurate predictions for maximal shortening and sub-maximal lengthening contractions respectively, and motivate advances in fields related to muscle modelling, the studies using these models however do not contribute to advancing the Hill-type modelling field itself.

Besides regular reviews that clarify the field and summarize its state-of-the-art, the field of Hill-type modelling would strongly benefit from globally-accepted recommendations, as proposed in other related fields (ESB recommendations). These could propose (1) standard definitions, notations and terminology for the common variables and dynamics of Hill-type models with respect to the chosen multiscale approach and rheological structure. As done for MSK systems (Hicks et al., 2015), those recommendations could provide a checklist and advise on (2) some best methodological practices, including the choice of mathematical metrics and experimental data for model validation, stating the assumptions and limitations related to the multiscale and rheological approaches, choosing the model complexity and completeness with regards to the study aim, taking the best approach for scaling and calibrating the model, and discussing its strengths and weaknesses in light of other findings in the literature. These recommendations should (3) refer to the sensitivity analyses in the field that have identified the most important model parameters, for which datasets compiling published experimental data for different species, muscles and scales should be produced for an optimized scaling of the models. Finally, they should provide (4a) a checklist of the details to include in the main manuscript or appendix for the full re-implementation of the model including the rheological structure, the equations describing the modelled properties, and a table listing the parameter values describing these properties and scaling the model, and (4b) suggest to modellers to release open-source implementations of their models so that the results presented in their study can be reproduced.

Conclusion

This study is the first systematic review of the field of Hill-type muscle-tendon modelling. The results of the completeness assessment (Figure 4 and Figure 5) describe the current trends and state-of-the-art in phenomenologically modelling 23 muscle properties in Hill-type systems. The results of the modelling assessment (Figure 6 and Figure 7) evaluate the current application of good practices in the field about model validation, reusability, modelling strategy and calibration. Supported by extensive supplementary material, global scores (Figure 8), and updated terminology (see Discussion Section and Table 1), this work is a convenient tool for scientists and modellers wishing to better understand the literature, choose the most suitable available model for their muscle-related study, or advance the state-of-the-art in Hill-type modelling. This study stresses the importance of contemporary reviews and global modelling recommendations to optimize inter-study consistency, knowledge transmission, and model reusability.

References

Abbott BC, Wilkie DR (1953) The relation between velocity of shortening and the tension-length curve of skeletal muscle. The Journal of physiology 120:214-223.

Ackland DC, Lin Y, Pandy MG (2012) Sensitivity of model predictions of muscle function to changes in moment arms and muscle–tendon properties: A monte-carlo analysis. J.Biomech. 45:1463-1471.

Ai Q, Ding B, Liu Q, Meng W (2016) A subject-specific EMG-driven musculoskeletal model for applications in lower-limb rehabilitation robotics. International journal of HR : humanoid robotics 13:1650005.

Akazawa K (2020) A novel hill-type two-mode model of skeletal muscle to simulate mechanisms underlying position control on the descending limb of the force–length relation. Advanced Biomedical Engineering 9:209-216.

Akazawa K (2019) A mathematical model of the dynamic force–length relationship of skeletal muscle operating on ascending and descending limbs. Advanced Biomedical Engineering 8:45-52.

Alcazar, J.,Csapo, R.,Ara, I.,Alegre, L.M.(2019) On the shape of the force-velocity relationship in skeletal muscles: The linear, the hyperbolic, and the double-hyperbolic. Front. Physiol., **10**.

Alizadeh M, Knapik GG, Mageswaran P, Mendel E, Bourekas E, Marras WS (2020) Biomechanical musculoskeletal models of the cervical spine: A systematic literature review. Clin.Biomech. 71:115-124.

Anderson FC, Pandy MG (1999) A dynamic optimization solution for vertical jumping in three dimensions. Computer methods in biomechanics and biomedical engineering 2:201-231.

Askew GN, Marsh RL (1998) Optimal shortening velocity (V/vmax) of skeletal muscle during cyclical contractions: Length-force effects and velocity-dependent activation and deactivation. J.Exp.Biol. 201:1527-1540.

Audu ML, Davy DT (1985) The influence of muscle model complexity in musculoskeletal motion modeling.

Bagni MA, Colombini B, Geiger P, Berlinguer Palmini R, Cecchi G (2004) Non-cross-bridge calcium-dependent stiffness in frog muscle fibers. American Journal of Physiology-Cell Physiology 286:C1353-C1357.

Bagni MA, Cecchi G, Colombini B, Colomo F (2002) A non-cross-bridge stiffness in activated frog muscle fibers. Biophys.J. 82:3118-3127.

Bahler AS (1968) Modeling of mammalian skeletal muscle. IEEE Transactions on Biomedical Engineering 249-257.

Balnave CD, Allen DG (1996) The effect of muscle length on intracellular calcium and force in single fibres from mouse skeletal muscle. J.Physiol.(Lond.) 492:705-713.

Barclay CJ, Curtin NA (2022) The legacy of AV hill's nobel prize winning work on muscle energetics. J.Physiol.(Lond.) 600:1555-1578.

Bayer, A.,Schmitt, S.,Günther, M.,Haeufle, D.F.B.(2017) The influence of biophysical muscle properties on simulating fast human arm movements. Computer Methods in Biomechanics and Biomedical Engineering, **20**, 803.

Baylor SM, Hollingworth S (2003) Sarcoplasmic reticulum calcium release compared in slow-twitch and fast-twitch fibres of mouse muscle. J.Physiol.(Lond.) 551:125-138.

Baylor SM, Hollingworth S (1998) Model of sarcomeric Ca2 movements, including ATP Ca2 binding and diffusion, during activation of frog skeletal muscle. J.Gen.Physiol. 112:297-316.

Baylor SM, Chandler WK, Marshall MW (1983) Sarcoplasmic reticulum calcium release in frog skeletal muscle fibres estimated from arsenazo III calcium transients. J.Physiol.(Lond.) 344:625-666.

Baylor SM, Hollingworth S (2012) Intracellular calcium movements during excitation–contraction coupling in mammalian slow-twitch and fast-twitch muscle fibers. J.Gen.Physiol. 139:261-272.

Baylor SM, Hollingworth S (2011) Calcium indicators and calcium signalling in skeletal muscle fibres during excitation–contraction coupling. Prog.Biophys.Mol.Biol. 105:162-179.

Bicer M, Phillips AT, Modenese L (2022) Altering the strength of the muscles crossing the lower limb joints only affects knee joint reaction forces. Gait Posture 95:210-216.

Bigland-Ritchie B, Kukulka CG, Lippold OC, Woods JJ (1982) The absence of neuromuscular transmission failure in sustained maximal voluntary contractions. J.Physiol.(Lond.) 330:265-278.

Blemker SS, Asakawa DS, Gold GE, Delp SL (2007) Image-based musculoskeletal modeling: Applications, advances, and future opportunities. Journal of Magnetic Resonance Imaging: An Official Journal of the International Society for Magnetic Resonance in Medicine 25:441-451.

Blemker SS, Delp SL (2005) Three-dimensional representation of complex muscle architectures and geometries. Ann.Biomed.Eng. 33:661-673.

Blinks JR, Rüdel R, Taylor SR (1978) Calcium transients in isolated amphibian skeletal muscle fibres: Detection with aequorin. J.Physiol.(Lond.) 277:291-323.

Blümel, M.,Guschlbauer, C.,Hooper, S.L.,Büschges, A.(2012) Using individual-muscle specific instead of across-muscle mean data halves muscle simulation error. Biol Cybern, **106**, 573.

Bobbert MF, van Ingen Schenau, Gerrit Jan (1990) Isokinetic plantar flexion: Experimental results and model calculations. Journal of biomechanics 23:105-119.

Bottinelli R, Pellegrino MA, Canepari M, Rossi R, Reggiani C (1999) Specific contributions of various muscle fibre types to human muscle performance: An in vitro study. Journal of Electromyography and Kinesiology 9:87-95.

Bottinelli R, Canepari M, Pellegrino MA, Reggiani C (1996) Force-velocity properties of human skeletal muscle fibres: Myosin heavy chain isoform and temperature dependence. J.Physiol.(Lond.) 495:573-586.

Brown IE, Cheng EJ, Loeb GE (1999) Measured and modeled properties of mammalian skeletal muscle. II. the effectsof stimulus frequency on force-length and force-velocity relationships. Journal of Muscle Research & Cell Motility 20:627-643.

Brynnel A, Hernandez Y, Kiss B, Lindqvist J, Adler M, Kolb J, van der Pijl R, Gohlke J, Strom J, Smith J, Ottenheijm C, Granzier HL (2018) Downsizing the molecular spring of the giant protein titin reveals that skeletal muscle titin determines passive stiffness and drives longitudinal hypertrophy. eLife 7:.

Bujalski P, Martins J, Stirling L (2018) A monte carlo analysis of muscle force estimation sensitivity to muscle-tendon properties using a hill-based muscle model. J.Biomech. 79:67-77.

Caggiano V, Wang H, Durandau G, Sartori M, Kumar V (2022) MyoSuite--A contact-rich simulation suite for musculoskeletal motor control. arXiv preprint arXiv:2205.13600 .

Caillet AH, Phillips AT, Farina D, Modenese L (2022) Estimation of the firing behaviour of a complete motoneuron pool by combining electromyography signal decomposition and realistic motoneuron modelling. PLOS Computational Biology 18:e1010556.

Caillet AH, Phillips AT, Farina D, Modenese L (2022) Mathematical relationships between spinal motoneuron properties. eLife 11:e76489.

Caldwell GE (1995) Tendon elasticity and relative length: Effects on the hill two-component muscle model. Journal of applied biomechanics 11:1-24.

Callahan DM, Umberger BR, Kent JA (2016) Mechanisms ofin vivomuscle fatigue in humans: Investigating age-related fatigue resistance with a computational model. The Journal of physiology 594:3407-3421.

Callahan DM, Umberger BR, Kent-Braun JA (2013) A computational model of torque generation: Neural, contractile, metabolic and musculoskeletal components. PloS one 8:e56013.

Camilleri MJ, Hull ML (2005) Are the maximum shortening velocity and the shape parameter in a hill-type model of whole muscle related to activation? J.Biomech. 38:2172-2180.

Campbell KS, Lakie M (1998) A cross-bridge mechanism can explain the thixotropic short-range elastic component of relaxed frog skeletal muscle. J.Physiol.(Lond.) 510:941-962.

Capote J, Bolaños P, Schuhmeier RP, Melzer W, Caputo C (2005) Calcium transients in developing mouse skeletal muscle fibres. J.Physiol.(Lond.) 564:451-464.

Carbone V, Van der Krogt, M M, Koopman HF, Verdonschot N (2016) Sensitivity of subject-specific models to hill muscle–tendon model parameters in simulations of gait. J.Biomech. 49:1953-1960.

Carriou V, Boudaoud S, Laforet J, Mendes A, Canon F, Guiraud D (2019) Multiscale hill-type modeling of the mechanical muscle behavior driven by the neural drive in isometric conditions. Computers in biology and medicine 115:103480.

Cheng EJ, Brown IE, Loeb GE (2000) Virtual muscle: A computational approach to understanding the effects of muscle properties on motor control. Journal of neuroscience methods 101:117-130.

Chow JW, Darling WG (1999) The maximum shortening velocity of muscle should be scaled with activation. J.Appl.Physiol. 86:1025-1031.

Close RI, Lännergren JI (1984) Arsenazo III calcium transients and latency relaxation in frog skeletal muscle fibres at different sarcomere lengths. J.Physiol.(Lond.) 355:323-344.

Cordo PJ, Rymer WZ (1982) Contributions of motor-unit recruitment and rate modulation of compensation for muscle yielding. J.Neurophysiol. 47:797-809.

Curtin NA, Gardner-Medwin AR, Woledge RC (1998) Predictions of the time course of force and power output by dogfish white muscle fibres during brief tetani. J.Exp.Biol. 201:103-114.

Dao TT, Tho MHB (2018) A systematic review of continuum modeling of skeletal muscles: Current trends, limitations, and recommendations. Applied bionics and biomechanics 2018:7631818-17.

De Groote F, Allen JL, Ting LH (2017) Contribution of muscle short-range stiffness to initial changes in joint kinetics and kinematics during perturbations to standing balance: A simulation study. J.Biomech. 55:71-77.

De Groote F, Kinney AL, Rao AV, Fregly BJ (2016) Evaluation of direct collocation optimal control problem formulations for solving the muscle redundancy problem. Ann.Biomed.Eng. 44:2922-2936.

De Groote F, Van Campen A, Jonkers I, De Schutter J (2010) Sensitivity of dynamic simulations of gait and dynamometer experiments to hill muscle model parameters of knee flexors and extensors. J.Biomech. 43:1876-1883.

Del Vecchio A, Holobar A, Falla D, Felici F, Enoka RM, Farina D (2020) Tutorial: Analysis of motor unit discharge characteristics from high-density surface EMG signals. Journal of Electromyography and Kinesiology 53:102426.

Delbono O, O'rourke KS, Ettinger WH (1995) Excitation-calcium release uncoupling in aged single human skeletal muscle fibers. J.Membr.Biol. 148:211-222.

Delbono O, Stefani E (1993) Calcium transients in single mammalian skeletal muscle fibres. J.Physiol.(Lond.) 463:689-707.

Delp SL, Anderson FC, Arnold AS, Loan P, Habib A, John CT, Guendelman E, Thelen DG (2007) OpenSim: Open-source software to create and analyze dynamic simulations of movement. TBME 54:1940-1950.

Delp SL, Loan JP, Hoy MG, Zajac FE, Topp EL, Rosen JM (1990) An interactive graphics-based model of the lower extremity to study orthopaedic surgical procedures. TBME 37:757-767.

Delp SL (1990) *Surgery Simulation: A Computer Graphics System to Analyze and Design Musculoskeletal Reconstructions of the Lower Limb.* Stanford University, .

Dembia CL, Bianco NA, Falisse A, Hicks JL, Delp SL (2020) Opensim moco: Musculoskeletal optimal control. PLOS Computational Biology 16:e1008493.

DeWoody Y, Martin CF, Schovanec L (2001) A forward dynamic model of gait with application to stress analysis of bone. Mathematical and computer modelling 33:121-143.

Dick TJM, Biewener AA, Wakeling JM (2017) Comparison of human gastrocnemius forces predicted by hill-type muscle models and estimated from ultrasound images. Journal of experimental biology 220:1643-1653.

Dideriksen JL, Negro F, Enoka RM, Farina D (2012) Motor unit recruitment strategies and muscle properties determine the influence of synaptic noise on force steadiness. Journal of Neurophysiology 107:3357-3369.

Dideriksen JL, Enoka RM, Farina D (2011) Neuromuscular adjustments that constrain submaximal EMG amplitude at task failure of sustained isometric contractions. Journal of Applied Physiology 111:485-494.

Dideriksen JL, Farina D, Baekgaard M, Enoka RM (2010) An integrative model of motor unit activity during sustained submaximal contractions. Journal of Applied Physiology 108:1550-1562.

Ding J, Wexler AS, Binder-Macleod SA (2000) Development of a mathematical model that predicts optimal muscle activation patterns by using brief trains. Journal of Applied Physiology 88:917-925.

Dorgan SJ, O'Malley MJ (1997) A nonlinear mathematical model of electrically stimulated skeletal muscle. T-RE 5:179-194.

Durfee WK, Palmer KI (1994) Estimation of force-activation, force-length, and force-velocity properties in isolated, electrically stimulated muscle. TBME 41:205-216.

Ebashi S, Endo M (1968) Calcium and muscle contraction. Prog.Biophys.Mol.Biol. 18:123-183.

Eckels EC, Haldar S, Tapia-Rojo R, Rivas-Pardo JA, Fernández JM (2019) The mechanical power of titin folding. Cell reports (Cambridge) 27:1836-1847.e4.

Edman KAP, Elzinga G, Noble MIM (1978) Enhancement of mechanical performance by stretch during tetanic contractions of vertebrate skeletal muscle fibres. J. Physiol. 218 139-155.

Edman KA (1988) Double-hyperbolic force-velocity relation in frog muscle fibres. J.Physiol.(Lond.) 404:301-321.

Edman KA (1979) The velocity of unloaded shortening and its relation to sarcomere length and isometric force in vertebrate muscle fibres. J.Physiol.(Lond.) 291:143-159.

Edman KAP (2005) Contractile properties of mouse single muscle fibers, a comparison with amphibian muscle fibers. Journal of Experimental Biology 208:1905-1913.

Eilenberg MF, Geyer H, Herr H (2010) Control of a powered ankle-foot prosthesis based on a neuromuscular model. TNSRE 18:164-173.

Elias LA, Watanabe RN, Kohn AF (2014) Spinal mechanisms may provide a combination of intermittent and continuous control of human posture: Predictions from a biologically based neuromusculoskeletal model. PLoS computational biology 10:e1003944.

Endo, M. (1973) Length dependence of activation of skinned muscle fibers by calcium. **37**, 505-510.

Epstein M (1998) Theoretical models of skeletal muscle: Biological and mathematical considerations. John Wiley & Sons 52-53.

Ettema GJ, Meijer K (2000) Muscle contraction history: Modified hill versus an exponential decay model. Biol.Cybern. 83:491-500.

Falisse A, Van Rossom S, Jonkers I, De Groote F (2016) EMG-driven optimal estimation of subject-specific hill model muscle–tendon parameters of the knee joint actuators. IEEE Transactions on Biomedical Engineering 64:2253-2262.

Farina D, Vujaklija I, Brånemark R, Bull AMJ, Dietl H, Graimann B, Hargrove LJ, Hoffmann K, Huang H, Ingvarsson T, Janusson HB, Kristjánsson K, Kuiken T, Micera S, Stieglitz T, Sturma A, Tyler D, Weir RFf, Aszmann OC (2021) Toward higher-performance bionic limbs for wider clinical use. Nature biomedical engineering 1-13.

Farina D, Vujaklija I, Sartori M, Kapelner T, Negro F, Jiang N, Bergmeister K, Andalib A, Principe J, Aszmann OC (2017) Man/machine interface based on the discharge timings of spinal motor neurons after targeted muscle reinnervation. Nature biomedical engineering 1:1-12.

Farina D, Negro F (2015) Common synaptic input to motor neurons, motor unit synchronization, and force control. Exerc.Sport Sci.Rev. 43:23-33.

Favier CD, Finnegan ME, Quest RA, Honeyfield L, McGregor AH, Phillips A (2021) An open-source musculoskeletal model of the lumbar spine and lower limbs: A validation for movements of the lumbar spine. Comput.Methods Biomech.Biomed.Engin. 24:1310-1325.

Favier CD, McGregor AH, Phillips AT (2021) Maintaining bone health in the lumbar spine: Routine activities alone are not enough. Frontiers in bioengineering and biotechnology 9:661837.

FitzHugh R (1977) A model of optimal voluntary muscular control. Journal of mathematical biology 4:203-236.

Frey Law LA, Shields RK (2006) Predicting human chronically paralyzed muscle force: A comparison of three mathematical models. Journal of Applied Physiology 100:1027-1036.

Fuglevand AJ, Winter DA, Patla AE (1993) Models of recruitment and rate coding organization in motor-unit pools. Journal of neurophysiology 70:2470-2488.

Fusi L, Brunello E, Yan Z, Irving M (2016) Thick filament mechano-sensing is a calcium-independent regulatory mechanism in skeletal muscle. Nature communications 7:1-9.

Gallucci JG, Challis JH (2002) Examining the role of the gastrocnemius during the leg curl exercise. Journal of Applied Biomechanics 18:15-27.

Getz EB, Cooke R, Lehman SL (1998) Phase transition in force during ramp stretches of skeletal muscle. Biophys.J. 75:2971-2983.

Geyer H, Herr H (2010) A muscle-reflex model that encodes principles of legged mechanics produces human walking dynamics and muscle activities. TNSRE 18:263-273.

Geyer H, Seyfarth A, Blickhan R (2003) Positive force feedback in bouncing gaits? Proceedings of the Royal Society of London.Series B: Biological Sciences 270:2173-2183.

Gfrerer MH, Simeon B (2021) Fiber-based modeling and simulation of skeletal muscles. Multibody system dynamics 52:1-30.

Giat Y, Mizrahi J, Levy M (1993) A musculotendon model of the fatigue profiles of paralyzed quadriceps muscle under FES. TBME 40:664-674.

Giat Y, Mizrahi J, Levine WS, Chen J (1994) Simulation of distal tendon transfer of the biceps brachii and the brachialis muscles. Journal of biomechanics 27:1005-1014.

Gittoes MJ, Brewin MA, Kerwin DG (2006) Soft tissue contributions to impact forces simulated using a four-segment wobbling mass model of forefoot–heel landings. Human movement science 25:775-787.

Godt RE, Maughan DW (1981) Influence of osmotic compression on calcium activation and tension in skinned muscle fibers of the rabbit. Pflügers Archiv 391:334-337.

Goislard de Monsabert B, Hauraix H, Caumes M, Herbaut A, Berton E, Vigouroux L (2020) Modelling force-length-activation relationships of wrist and finger extensor muscles. Med.Biol.Eng.Comput. 58:2531-2549.

Gollapudi SK, Lin DC (2009) Experimental determination of sarcomere force–length relationship in type-I human skeletal muscle fibers. J.Biomech. 42:2011-2016.

Gömmel A, Butenweg C, Bolender K, Grunendahl A (2007) A muscle controlled finite-element model of laryngeal abduction and adduction. Computer methods in biomechanics and biomedical engineering 10:377-388.

Gordon, Huxley, Julian (1966) The variation in isometric tension with sarcomere length in vertebrate muscle fibres. The Journal of physiology 184:170-192.

Granzier HL, Burns DH, Pollack GH (1989) Sarcomere length dependence of the force-velocity relation in single frog muscle fibers. Biophys.J. 55:499-507.

Gruber K, Ruder H, Denoth J, Schneider K (1998) A comparative study of impact dynamics: Wobbling mass model versus rigid body models. J.Biomech. 31:439-444.

Guimaraes AC, Herzog W, Hulliger M, Zhang YT, Day S (1994) Effects of muscle length on the EMG-force relationship of the cat soleus muscle studied using non-periodic stimulation of ventral root filaments. J.Exp.Biol. 193:49-64.

Günther M, Haeufle DFB, Schmitt S (2018) The basic mechanical structure of the skeletal muscle machinery: One model for linking microscopic and macroscopic scales. Journal of theoretical biology 456:137-167.

Günther, M.,Schmitt, S.,Wank, V.(2007) High-frequency oscillations as a consequence of neglected serial damping in hill-type muscle models. Biol Cybern, **97**, 63.

Guo J, Sun Y, Hao Y, Cui L, Ren G (2020) A mass-flowing muscle model with shape restrictive soft tissues: Correlation with sonoelastography. Biomechanics and modeling in mechanobiology 19:911-926.

Hamburger, A. (2017) Comparison between different muscular models. http://hdl.handle.net/2078.1/thesis:10689.

Hamouda A, Kenney L, Howard D (2016) Dealing with time-varying recruitment and length in hill-type muscle models. Journal of biomechanics 49:3375-3380.

Handsfield GG, Meyer CH, Hart JM, Abel MF, Blemker SS (2014) Relationships of 35 lower limb muscles to height and body mass quantified using MRI. J.Biomech. 47:631-638.

Happee R (1994) Inverse dynamic optimization including muscular dynamics, a new simulation method applied to goal directed movements. J.Biomech. 27:953-960.

Hassani W, Mohammed S, Rifaï H, Amirat Y (2014) Powered orthosis for lower limb movements assistance and rehabilitation. Control Eng.Pract. 26:245-253.

Hasson, C. J.,Caldwell, G.E.(2011) Effects of age on mechanical properties of dorsiflexor and plantarflexor muscles. Ann Biomed Eng, **40**, 1088.

Hatze H (1981) Estimation of myodynamic parameter values from observations on isometrically contracting muscle groups. European journal of applied physiology and occupational physiology 46:325-338.

Hatze H (1980) *Myocybernetic Control Models of Skeletal Muscle - Characteristics and Applications.* University of South Africa Press, Pretoria, .

Hatze H (1977) A myocybernetic control model of skeletal muscle. Biological cybernetics 25:103-119.

Hatze H (1978) A general myocybernetic control model of skeletal muscle. Biological Cybernetics 28 143-157.

He J. | Levine W.S. | Loeb G.E. (1991) *Feedback Gains for Correcting Small Perturbations to Standing Posture.* Automatic Control, IEEE Transactions, .

He J, Levine WS, Loeb GE (1991) Feedback gains for correcting small perturbations to standing posture. TAC 36:322-332.

Heckman CJ, Binder MD (1991) Computer simulation of the steady-state input-output function of the cat medial gastrocnemius motoneuron pool. J.Neurophysiol. 65:952-967.

Heckman CJ, Enoka RM (2012) Motor unit. Compr. Physiol. 2:2629-2682.

Heidlauf, T.,Klotz,Rode,Siebert, T.,Röhrle, O.(2017) A continuum-mechanical skeletal muscle model including actin-titin interaction predicts stable contractions on the descending limb of the force-length relation.

Heidlauf T, Röhrle O (2014) A multiscale chemo-electro-mechanical skeletal muscle model to analyze muscle contraction and force generation for different muscle fiber arrangements. Frontiers in physiology 5:498.

Henneman E (1985) The size-principle: A deterministic output emerges from a set of probabilistic connections. J. Exp. Biol. 115:105-112.

Henneman E (1981) Recruitment of motoneurons : The size principle. Motor Unit Types, Recruitment and Plasticity in Health and Disease 26-60.

Henneman E (1957) Relation between size of neurons and their susceptibility to discharge. Science 126:1345-1347.

Herzog W, Schappacher G, DuVall M, Leonard TR, Herzog JA (2016) Residual force enhancement following eccentric contractions: A new mechanism involving titin. Physiology (Bethesda, Md.) 31:300-312.

Herzog, W., Joumaa, V. & Leonard, T. R. (2010) The Force–Length relationship of mechanically isolated sarcomeres. In Anonymous *Muscle Biophysics.* Springer New York, New York, NY, pp. 141-161.

Herzog W (2019) The problem with skeletal muscle series elasticity. BMC biomedical engineering 1:28.

Herzog W, Powers K, Johnston K, Duvall M (2015) A new paradigm for muscle contraction. Frontiers in physiology 6:174.

Hessel AL, Lindstedt SL, Nishikawa KC (2017) Physiological mechanisms of eccentric contraction and its applications: A role for the giant titin protein. Frontiers in physiology 8:70.

Hicks JL, Uchida TK, Seth A, Rajagopal A, Delp SL (2015) Is my model good enough? best practices for verification and validation of musculoskeletal models and simulations of movement. J.Biomech.Eng. 137:.

Hill (1938) The heat of shortening and the dynamic constants of muscle. Series B-Biological Sciences 126(843):136-195.

Hill (1922) The maximum work and mechanical efficiency of human muscles, and their most economical speed. J.Physiol.(Lond.) 56:19.

Hirota A, Chandler WK, Southwick PL, Waggoner AS (1989) Calcium signals recorded from two new purpurate indicators inside frog cut twitch fibers. J.Gen.Physiol. 94:597-631.

Hof AL, Van den Berg J (1981) EMG to force processing I: An electrical analogue of the hill muscle model. Journal of biomechanics 14:747,755-753,758.

Holash RJ, MacIntosh BR (2019) A stochastic simulation of skeletal muscle calcium transients in a structurally realistic sarcomere model using MCell. PLoS Computational Biology 15:e1006712.

Hollingworth S, Zhao M, Baylor SM (1996) The amplitude and time course of the myoplasmic free [Ca2] transient in fast-twitch fibers of mouse muscle. J.Gen.Physiol. 108:455-469.

Hollingworth S, Kim MM, Baylor SM (2012) Measurement and simulation of myoplasmic calcium transients in mouse slow-twitch muscle fibres. J.Physiol.(Lond.) 590:575-594.

Hollingworth S, Zeiger U, Baylor SM (2008) Comparison of the myoplasmic calcium transient elicited by an action potential in intact fibres of mdx and normal mice. J.Physiol.(Lond.) 586:5063-5075.

Holt NC, Azizi E (2014) What drives activation-dependent shifts in the force–length curve? Biology letters 10:20140651.

Hou M (2018) Force–length relation of skeletal muscles: From sarcomeres to myofibril. Biomechanics and Modeling in Mechanobiology 17:1797-1810.

Houdijk H, Bobbert MF, de Haan A (2006) Evaluation of a hill based muscle model for the energy cost and efficiency of muscular contraction. Journal of biomechanics 39:536-543.

Huijing, P. A. & Slawnych, M. P. (2000) Modeling of homogeneous muscle: Is it realistic to consider skeletal muscle as a lumped sarcomere or fiber? In Anonymous *Biomechanics and Neural Control of Posture and Movement.* Springer, pp. 92-99.

Huijing PA (1999) Muscle as a collagen fiber reinforced composite: A review of force transmission in muscle and whole limb. J.Biomech. 32:329-345.

Huijing PA (1996) Important experimental factors for skeletal muscle modelling: Non-linear changes of muscle length force characteristics as a function of degree of activity. Eur.J.Morphol. 34:47-54.

Hussein M, Shebl S, Elnemr R, Elkaranshawy H (2022) A new muscle activation dynamics model, that simulates the calcium kinetics and incorporates the role of store-operated calcium entry channels, to enhance the electromyography-driven hill-type models. J.Biomech.Eng. 144:.

Huxley, Hanson (1954) Changes in the cross-striations of muscle during contraction and stretch and their structural interpretation. Nature 173:973-976.

Huxley, Niedergerke (1954) Structural changes in muscle during contraction: Interference microscopy of living muscle fibres. Nature 173:971-973.

John CT, Anderson FC, Higginson JS, Delp SL (2013) Stabilisation of walking by intrinsic muscle properties revealed in a three-dimensional muscle-driven simulation. Comput.Methods Biomech.Biomed.Engin. 16:451-462.

Joyce GC, Rack P, Westbury DR (1969) The mechanical properties of cat soleus muscle during controlled lengthening and shortening movements. J.Physiol.(Lond.) 204:461-474.

Julian FJ (1969) Activation in a skeletal muscle contraction model with a modification for insect fibrillar muscle. Biophys.J. 9:547-570.

Kapelner T, Sartori M, Negro F, Farina D (2020) Neuro-musculoskeletal mapping for man-machine interfacing. Scientific reports 10:1-10.

Kearney KM, Harley JB, Nichols JA (2021) Classifying muscle parameters with artificial neural networks and simulated lateral pinch data. Plos one 16:e0255103.

Kian A, Pizzolato C, Halaki M, Ginn K, Lloyd D, Reed D, Ackland D (2021) The effectiveness of EMG-driven neuromusculoskeletal model calibration is task dependent. J.Biomech. 129:110698.

Kim H, Kim M (2018) PyMUS: Python-based simulation software for virtual experiments on motor unit system. Frontiers in neuroinformatics 12:15.

Kim, H.,Sandercock, T.G.,Heckman, C.J.(2015) An action potential-driven model of soleus muscle activation dynamics for locomotor-like movements. J. Neural Eng., **12**.

Kistemaker DA, Van Soest, Arthur (Knoek) J, Bobbert MF (2006) Is equilibrium point control feasible for fast goal-directed single-joint movements? J.Neurophysiol. 95:2898-2912.

Klein CS, Rice CL, Marsh GD (2001) Normalized force, activation, and coactivation in the arm muscles of young and old men. J.Appl.Physiol. 91:1341-1349.

Konishi M, Hollingworth S, Harkins AB, Baylor SM (1991) Myoplasmic calcium transients in intact frog skeletal muscle fibers monitored with the fluorescent indicator furaptra. J.Gen.Physiol. 97:271-301.

Kovyazina IV, Tsentsevitsky AN, Nikolsky EE, Bukharaeva EA (2010) Kinetics of acetylcholine quanta release at the neuromuscular junction during high-frequency nerve stimulation. Eur.J.Neurosci. 32:1480-1489.

Lee SSM, Arnold AS, Miara MdB, Biewener AA, Wakeling JM (2013) Accuracy of gastrocnemius muscles forces in walking and running goats predicted by one-element and two-element hill-type models. Journal of biomechanics 46:2288-2295.

Legreneur P, Morlon B, Van Hoecke J (1996) Simulation of in situ soleus isometric force output as a function of neural excitation. Journal of biomechanics 29:1455-1462.

Lemaire KK, Baan GC, Jaspers RT, van Soest, A J 'Knoek' (2016) Comparison of the validity of hill and huxley muscle-tendon complex models using experimental data obtained from rat m. soleus in situ. Journal of experimental biology 219:2228.

Li Y, Unger A, von Frieling-Salewsky M, Pardo JAR, Fernandez JM, Linke WA (2018) Quantifying the titin contribution to muscle force generation using a novel method to specifically cleave the titin springs in situ. Biophys.J. 114:645a.

Lichtwark GA, Bougoulias K, Wilson AM (2007) Muscle fascicle and series elastic element length changes along the length of the human gastrocnemius during walking and running. J.Biomech. 40:157-164.

Liu JZ, Brown RW, Yue GH (2002) A dynamical model of muscle activation, fatigue, and recovery. Biophysical journal 82:2344-2359.

Liu W, Nigg BM (2000) A mechanical model to determine the influence of masses and mass distribution on the impact force during running. J.Biomech. 33:219-224.

Lloyd DG, Besier TF (2003) An EMG-driven musculoskeletal model to estimate muscle forces and knee joint moments in vivo. Journal of Biomechanics 36:765-776.

Maceri F, Maceri F, Marino M, Marino M, Vairo G, Vairo G (2012) An insight on multiscale tendon modeling in muscle–tendon integrated behavior. Biomech Model Mechanobiol 11:505-517.

Malamud JG, Godt RE, Nichols TR (1996) Relationship between short-range stiffness and yielding in type-identified, chemically skinned muscle fibers from the cat triceps surae muscles. J.Neurophysiol. 76:2280-2289.

Manal K, Gonzalez RV, Lloyd DG, Buchanan TS (2002) A real-time EMG-driven virtual arm. Computers in biology and medicine 32:25-36.

Marcucci L, Reggiani C, Natali AN, Pavan PG (2017) From single muscle fiber to whole muscle mechanics: A finite element model of a muscle bundle with fast and slow fibers. Biomechanics and modeling in mechanobiology 16:1833-1843.

Mashima H, AKAZAWA K, KUSHIMA H, FUJII K (1972) The force-load-velocity relation and the viscous-like force in the frog skeletal muscle. The Japanese journal of physiology 22:103-120.

Matsuo T, Iwamoto H, Yagi N (2010) Monitoring the structural behavior of troponin and myoplasmic free Ca2 concentration during twitch of frog skeletal muscle. Biophys.J. 99:193-200.

Mavritsaki, E.,Lepora, N.,Porrill, J.,Yeo, C.H.,Dean, P.(2007) Response linearity determined by recruitment strategy in detailed model of nictitating membrane control. Biol Cybern, **96**, 39.

McDonald KS, Blaser CA, Fitts RH (1994) Force-velocity and power characteristics of rat soleus muscle fibers after hindlimb suspension. J.Appl.Physiol. 77:1609-1616.

McLean SG, Su A, van den Bogert, Antonie J (2003) Development and validation of a 3-D model to predict knee joint loading during dynamic movement. J.Biomech.Eng. 125:864-874.

Meijer, K.,Meijer, K.,Grootenboer, H.J.,Koopman, H F J M,Van Der Linden, B J J J,Huijing, P.A.(1998) Application of wearable sensors view project A hill type model of rat medial gastrocnemius muscle that accounts for shortening history effects. Article in Journal of Biomechanics, **31**, 555.

Menegaldo LL, Oliveira LFd (2009) Effect of muscle model parameter scaling for isometric plantar flexion torque prediction. Journal of biomechanics 42:2597-2601.

Michaud F, Lamas M, Lugrís U, Cuadrado J (2021) A fair and EMG-validated comparison of recruitment criteria, musculotendon models and muscle coordination strategies, for the inverse-dynamics based optimization of muscle forces during gait. Journal of neuroengineering and rehabilitation 18:17.

Millard M, Uchida T, Seth A, Delp SL (2013) Flexing computational muscle: Modeling and simulation of musculotendon dynamics. Journal of biomechanical engineering 135:021005.

Modenese L, Kohout J (2020) Automated generation of three-dimensional complex muscle geometries for use in personalised musculoskeletal models. Ann.Biomed.Eng. 48:1793-1804.

Modenese L, Ceseracciu E, Reggiani M, Lloyd DG (2016) Estimation of musculotendon parameters for scaled and subject specific musculoskeletal models using an optimization technique. J.Biomech. 49:141-148.

Moher D, Liberati A, Tetzlaff J, Altman DG, PRISMA Group* (2009) Preferred reporting items for systematic reviews and meta-analyses: The PRISMA statement. Ann.Intern.Med. 151:264-269.

Moisescu DG, Thieleczek R (1979) Sarcomere length effects on the Sr2 -and Ca2 -activation curves in skinned frog muscle fibres. Biochim.Biophys.Acta 546:64-76.

Monte, A.,Baltzopoulos, V.,Maganaris, C.N.,Zamparo, P.(2020) Gastrocnemius medialis and vastus lateralis in vivo muscle-tendon behavior during running at increasing speeds. Scand J Med Sci Sports, **30**, 1163.

Moo EK, Leonard TR, Herzog W (2020) The sarcomere force–length relationship in an intact muscle–tendon unit. J.Exp.Biol. 223:jeb215020.

Moody, C. B.,Barhorst, A.A.,Schovanec, L.(2009) A neuro-muscular elasto-dynamic model of the human arm part 2: Musculotendon dynamics and related stress effects. J Bionic Eng, **6**, 108.

Mörl, F.,Siebert, T.,Schmitt, S.,Blickhan, R.,Günther, M.(2012) Electro-mechanical delay in hill-type muscle models. J. Mech. Med. Biol., **12**.

Moss RL (1986) Effects on shortening velocity of rabbit skeletal muscle due to variations in the level of thin-filament activation. J.Physiol.(Lond.) 377:487-505.

Muceli S, Poppendieck W, Holobar A, Gandevia S, Liebetanz D, Farina D (2022) Accurate decoding of the spinal cord output in humans with implanted high-density electrode arrays. bioRxiv .

Neidhard-Doll AT, Phillips CA, Repperger DW, Reynolds DB (2004) Biomimetic model of skeletal muscle isometric contraction: II. A phenomenological model of the skeletal muscle excitation–contraction coupling process. Comput.Biol.Med. 34:323-344.

Nichols, T. R. (1984) Velocity sensitivity of yielding during stretch in the cat soleus muscle. In Anonymous *Contractile Mechanisms in Muscle.* Springer, pp. 753-755.

Nikooyan AA, Veeger HEJ, Westerhoff P, Bolsterlee B, Graichen F, Bergmann G, van der Helm FCT (2012) An EMG-driven musculoskeletal model of the shoulder. Human movement science 31:429-447.

Niu, C. M.,Luo, Q.I.,Chou, C.,Liu, J.,Hao, M.,Lan, N.(2020) Neuromorphic model of reflex for realtime human-like compliant control of prosthetic hand. Ann Biomed Eng, **49**, 673.

Nussbaum MA, Chaffin DB (1998) Lumbar muscle force estimation using a subject-invariant 5-parameter EMG-based model. J.Biomech. 31:667-672.

Otten E (1987) A myocybernetic model of the jaw system of the rat. Journal of Neuroscience Methods 21:287-302.

Pain MT, Challis JH (2006) The influence of soft tissue movement on ground reaction forces, joint torques and joint reaction forces in drop landings. J.Biomech. 39:119-124.

Pandy MG, Zajac FE, Sim E, Levine WS (1990) An optimal control model for maximum-height human jumping. Journal of biomechanics 23:1185-1198.

Penasso H, Thaller S (2018) Model-based analysis of fatigued human knee extensors. Eur.J.Appl.Physiol. 118:1447-1461.

Peng, L.,Hou, Z.,Peng, L.,Wang, W.(2016) Experimental study of robot-assisted exercise training for knee rehabilitation based on a practical EMG-driven model. , 810-814.

Perreault EJ, Heckman CJ, Sandercock TG (2003) Hill muscle model errors during movement are greatest within the physiologically relevant range of motor unit firing rates. J.Biomech. 36:211-218.

Petersen E, Rostalski P (2019) A comprehensive mathematical model of motor unit pool organization, surface electromyography, and force generation. Frontiers in physiology 10:176.

Petrofsky JS, Phillips CA (1981) The influence of temperature, initial length and electrical activity on the force-velocity relationship of the medial gastrocnemius muscle of the cat. J.Biomech. 14:297-306.

Phillips AT, Villette CC, Modenese L (2015) Femoral bone mesoscale structural architecture prediction using musculoskeletal and finite element modelling. International Biomechanics 2:43-61.

Piazzesi G, Caremani M, Linari M, Reconditi M, Lombardi V (2018) Thick filament mechano-sensing in skeletal and cardiac muscles: A common mechanism able to adapt the energetic cost of the contraction to the task. Frontiers in physiology 9:736.

Pierrynowski MR, Morrison JB (1985) A physiological model for the evaluation of muscular forces in human locomotion: Theoretical aspects. Math.Biosci. 75:69-101.

Pizarro G, Olivera JF (2020) The dynamics of Ca2 within the sarcoplasmic reticulum of frog skeletal muscle. A simulation study. J.Theor.Biol. 504:110371.

Potvin JR, Fuglevand AJ (2017) A motor unit-based model of muscle fatigue. PLoS computational biology 13:e1005581.

Powers K, Schappacher-Tilp G, Jinha A, Leonard T, Nishikawa K, Herzog W (2014) Titin force is enhanced in actively stretched skeletal muscle. J.Exp.Biol. 217:3629-3636.

Prado LG, Makarenko I, Andresen C, Krüger M, Opitz CA, Linke WA (2005) Isoform diversity of giant proteins in relation to passive and active contractile properties of rabbit skeletal muscles. J.Gen.Physiol. 126:461-480.

Proctor, J.,Holmes, P.P.(2010) Reflexes and preflexes: On the role of sensory feedback on rhythmic patterns in insect locomotion. Biol Cybern, **102**, 513.

Putra, I. P. A.,Carmai, J.,Koetniyom, S.,Markert, B.(2015) The effects of active muscle contraction into pedestrian kinematics and injury during vehicle-pedestrian collision.

Rack PM, Westbury DR (1969) The effects of length and stimulus rate on tension in the isometric cat soleus muscle. J.Physiol.(Lond.) 204:443.

Raikova R, Celichowski J, Angelova S, Krutki P (2018) A model of the rat medial gastrocnemius muscle based on inputs to motoneurons and on an algorithm for prediction of the motor unit force. Journal of neurophysiology 120:1973-1987.

Rajagopal A, Dembia CL, DeMers MS, Delp DD, Hicks JL, Delp SL (2016) Full-body musculoskeletal model for muscle-driven simulation of human gait. TBME 63:2068-2079.

Raju B, Murphy E, Levy LA, Hall RD, London RE (1989) A fluorescent indicator for measuring cytosolic free magnesium. American Journal of Physiology-Cell Physiology 256:C540-C548.

Ranatunga KW (1982) Temperature-dependence of shortening velocity and rate of isometric tension development in rat skeletal muscle. J.Physiol.(Lond.) 329:465-483.

Rasmussen, J.,Damsgaard, M.,Surma, E.,Christensen, S.T.,de Zee, M.,Vondrak, V.(2003) Anybody-a software system for ergonomic optimization. **4**, 6.

Rasmussen J, Vondrak V, Damsgaard M, De Zee M, Christensen ST, Dostal Z (2002) The anybody project–computer analysis of the human body. Biomechanics of Man 270-274.

Rassier DE, Leite FS, Nocella M, Cornachione AS, Colombini B, Bagni MA (2015) Non-crossbridge forces in activated striated muscles: A titin dependent mechanism of regulation? J.Muscle Res.Cell.Motil. 36:37-45.

Rassier DE, MacIntosh BR, Herzog W (1999) Length dependence of active force production in skeletal muscle. J.Appl.Physiol. 86:1445-1457.

Redl C, Gfoehler M, Pandy MG (2007) Sensitivity of muscle force estimates to variations in muscle–tendon properties. Human movement science 26:306-319.

Rengifo C, Aoustin Y, Plestan F, Chevallereau C (2010) Distribution of forces between synergistics and antagonistics muscles using an optimization criterion depending on muscle contraction behavior. J Biomech Eng 132:041009.

Riener R, Fuhr T (1998) Patient-driven control of FES-supported standing up: A simulation study. IEEE Transactions on rehabilitation engineering 6:113-124.

Riener R, Quintern J, Schmidt G (1996) Biomechanical model of the human knee evaluated by neuromuscular stimulation. J.Biomech. 29:1157-1167.

Rivas-Pardo J, Eckels E, Popa I, Kosuri P, Linke W, Fernández J (2016) Work done by titin protein folding assists muscle contraction. Cell reports (Cambridge) 14:1339-1347.

Rockenfeller R, Herold JL, Götz T (2020) Parameter estimation and experimental design for hill-type muscles: Impulses from optimization-based modeling. Mathematical biosciences 327:108432.

Rockenfeller, R., & Günther, M. (2017a). Hill equation and Hatze's muscle activation dynamics complement each other: enhanced pharmacological and physiological interpretability of modelled activity-pCa curves. Journal of Theoretical Biology, 431, 11-24.

Rockenfeller R, Günther M (2017b) How to model a muscle's active force–length relation: A comparative study. Computer Methods in Applied Mechanics and Engineering 313:321-336.

Rockenfeller R, Günther M (2018) Inter-filament spacing mediates calcium binding to troponin: A simple geometric-mechanistic model explains the shift of force-length maxima with muscle activation. Journal of theoretical biology 454:240-252.

Rockenfeller, R., Günther, M., & Hooper, S. L. (2022). Muscle active force-length curve explained by an electrophysical model of interfilament spacing. Biophysical Journal, 121(10), 1823-1855.

Rode C, Siebert T, Blickhan R (2009) Titin-induced force enhancement and force depression: A 'sticky-spring' mechanism in muscle contractions? Journal of theoretical biology 259:350-360.

Röhrle O, Davidson JB, Pullan AJ (2012) A physiologically based, multi-scale model of skeletal muscle structure and function. Frontiers in physiology 3:358.

Röhrle, O.,Yavuz, U.Ş,Klotz, T.,Negro, F.,Heidlauf, T., K E Y W O R D S(2019) Organ, tissue, and physiological models. WIREs Syst Biol Med, .

Röhrle O, Yavuz U, Klotz T, Negro F, Heidlauf T (2019) Multiscale modeling of the neuromuscular system: Coupling neurophysiology and skeletal muscle mechanics. Wiley interdisciplinary reviews. Systems biology and medicine 11:e1457.

Roots H, Offer GW, Ranatunga KW (2007) Comparison of the tension responses to ramp shortening and lengthening in intact mammalian muscle fibres: Crossbridge and non-crossbridge contributions. J.Muscle Res.Cell.Motil. 28:123-139.

Ross SA, Rimkus B, Konow N, Biewener AA, Wakeling JM (2020) Added mass in rat plantaris muscle causes a reduction in mechanical work. J.Exp.Biol. 223:jeb224410.

Ross, S. A.,Nigam, N.,Wakeling, J.M.(2018) A modelling approach for exploring muscle dynamics during cyclic contractions.

Ross SA, Ryan DS, Dominguez S, Nigam N, Wakeling JM (2018) Size, history-dependent, activation and three-dimensional effects on the work and power produced during cyclic muscle contractions. Integrative and comparative biology 58:232-250.

Ross SA, Wakeling JM (2016) Muscle shortening velocity depends on tissue inertia and level of activation during submaximal contractions. Biology letters 12:20151041.

Sarshari, E.,Mancuso, M.,Terrier, A.,Farron, A.,Mullhaupt, P.,Pioletti, D.(2020) Muscle co-contraction in an upper limb musculoskeletal model: EMG-assisted vs. standard load-sharing. Computer Methods in Biomechanics and Biomedical Engineering, **24**, 137.

Sartori M, Yavuz U, Farina D (2017) In vivo neuromechanics: Decoding causal motor neuron behavior with resulting musculoskeletal function. Scientific reports 7:13465-14.

Sartori M, Reggiani M, Farina D, Lloyd DG (2012) EMG-driven forward-dynamic estimation of muscle force and joint moment about multiple degrees of freedom in the human lower extremity. PloS one 7:e52618.

Schappacher-Tilp G (2018) Titin-mediated thick filament activation stabilizes myofibrils on the descending limb of their force–length relationship. Journal of Sport and Health Science 7:326-332.

Schappacher-Tilp G, Leonard T, Desch G, Herzog W (2015) A novel three-filament model of force generation in eccentric contraction of skeletal muscles. PloS one 10:e0117634.

Schmitt S, Günther M, Häufle DFB (2019) The dynamics of the skeletal muscle: A systems biophysics perspective on muscle modeling with the focus on hill-type muscle models. Mitteilungen der Gesellschaft für Angewandte Mathematik und Mechanik 42:n/a.

Schutte LM, Rodgers MM, Zajac FE, Glaser RM (1993) Improving the efficacy of electrical stimulation-induced leg cycle ergometry: An analysis based on a dynamic musculoskeletal model. IEEE Transactions on Rehabilitation Engineering 1:109-125.

Scott SH, Winter DA (1991) A comparison of three muscle pennation assumptions and their effect on isometric and isotonic force. J.Biomech. 24:163-167.

Scovil CY, Ronsky JL (2006) Sensitivity of a hill-based muscle model to perturbations in model parameters. Journal of biomechanics 39:2055-2063.

Seiberl W, Paternoster F, Achatz F, Schwirtz A, Hahn D (2013) On the relevance of residual force enhancement for everyday human movement. J.Biomech. 46:1996-2001.

Seth A, Hicks JL, Uchida TK, Habib A, Dembia CL, Dunne JJ, Ong CF, Demers MS, Rajagopal A, Millard M, Hamner SR, Arnold EM (2018) OpenSim: Simulating musculoskeletal dynamics and neuromuscular control to study human and animal movement. PLoS computational biology 14:e1006223.

Shao Q, Bassett DN, Manal K, Buchanan TS (2009) An EMG-driven model to estimate muscle forces and joint moments in stroke patients. Computers in biology and medicine 39:1083-1088.

Sharma, N.,Patre, P.M.,Gregory, C.M.,Dixon, W.E.(Jan 01, 2009) Nonlinear control of NMES: Incorporating fatigue and calcium dynamics. ASME 2009 Dynamic Systems and Control Conference, Volume 1, , 705-712. https://asmedigitalcollection.asme.org/DSCC/proceedings/DSCC2009/48920/705/346404.

Shorten PR, O'Callaghan P, Davidson JB, Soboleva TK (2007) A mathematical model of fatigue in skeletal muscle force contraction. J.Muscle Res.Cell.Motil. 28:293-313.

Shue G, Crago P (1998) Muscle–Tendon model with length history-dependent Activation–Velocity coupling. Annals of Biomedical Engineering 26:369-380.

Siebert T, Stutzig N, Rode C (2018) A hill-type muscle model expansion accounting for effects of varying transverse muscle load. Journal of biomechanics 66:57-62.

Siebert T, Siebert T, Rode C, Rode C, Herzog W, Herzog W, Till O, Till O, Blickhan R, Blickhan R (2008) Nonlinearities make a difference: Comparison of two common hill-type models with real muscle. Biol Cybern 98:133-143.

Smith, N. P.,Barclay, C.J.,Loiselle, D.S.(2005) The efficiency of muscle contraction. Progress in Biophysics and Molecular Biology, **88**, 1-58. https://dx.doi.org/10.1016/j.pbiomolbio.2003.11.014.

Song D, Raphael G, Lan N, Loeb GE (2008) Computationally efficient models of neuromuscular recruitment and mechanics. Journal of Neural Engineering 5:175.

Stelzer M, Von Stryk O (2006) Efficient forward dynamics simulation and optimization of human body dynamics. ZAMM-Journal of Applied Mathematics and Mechanics/Zeitschrift für Angewandte Mathematik und Mechanik: Applied Mathematics and Mechanics 86:828-840.

Stephenson DG, Wendt IR (1984) Length dependence of changes in sarcoplasmic calcium concentration and myofibrillar calcium sensitivity in striated muscle fibres. Journal of Muscle Research & Cell Motility 5:243-272.

Stephenson DG, Williams DA (1982) Effects of sarcomere length on the force—pCa relation in fast- and slow-twitch skinned muscle fibres from the rat. J.Physiol.(Lond.) 333:637-653.

Sun L, Sun Y, Huang Z, Hou J, Wu J (2018) Improved hill-type musculotendon models with activation-force-length coupling. Technology and Health Care 26:909-920.

Sutarno CG, McGill SM (1995) Isovelocity investigation of the lengthening behaviour of the erector spinae muscles. Eur.J.Appl.Physiol.Occup.Physiol. 70:146-153.

Tahir U, Monroy JA, Rice NA, Nishikawa KC (2020) Effects of a titin mutation on force enhancement and force depression in mouse soleus muscles. J.Exp.Biol. 223:jeb197038.

Tamura Y, Saito M, Ito A (2008) The phenomenological model of muscle contraction with a controller to simulate the excitation–contraction (E–C) coupling. Journal of biomechanics 42:400-403.

Thelen, D. G. (2003) Adjustment of muscle mechanics model parameters to simulate dynamic contractions in older adults. Journal of biomechanical engineering, **125**, 70. https://www.ncbi.nlm.nih.gov/pubmed/12661198.

Thompson CK, Negro F, Johnson MD, Holmes MR, McPherson LM, Powers RK, Farina D, Heckman CJ (2018) Robust and accurate decoding of motoneuron behaviour and prediction of the resulting force output. J.Physiol.(Lond.) 596:2643-2659.

Tigue JA, Rockwell WB, Foreman KB, Mascaro SA (2022) Investigating the effects of flexor tendon shortening on active range of motion after finger tendon repair. Anat.Rec. 305:1231-1244.

Till O, Siebert T, Rode C, Blickhan R (2008) Characterization of isovelocity extension of activated muscle: A hill-type model for eccentric contractions and a method for parameter determination. Journal of theoretical biology 255:176-187.

Trinler U, Hollands K, Jones R, Baker R (2018) A systematic review of approaches to modelling lower limb muscle forces during gait: Applicability to clinical gait analyses. Gait Posture 61:353-361.

Tsianos GA, Rustin C, Loeb GE (2011) Mammalian muscle model for predicting force and energetics during physiological behaviors. IEEE Transactions on Neural Systems and Rehabilitation Engineering 20:117-133.

Van Den Bogert, Antonie J, Blana D, Heinrich D (2011) Implicit methods for efficient musculoskeletal simulation and optimal control. Procedia Iutam 2:297-316.

van Ingen Schenau, G J, Bobbert MF, Ettema GJ, De Graaf JB, Huijing PA (1988) A simulation of rat EDL force output based on intrinsic muscle properties. J.Biomech. 21:815-824.

Van Ruijven LJ, Weijs WA (1990) A new model for calculating muscle forces from electromyograms. Eur.J.Appl.Physiol.Occup.Physiol. 61:479-485.

van Soest AJ, Bobbert MF (1993) The contribution of muscle properties in the control of explosive movements. Biol.Cybern. 69:195-204.

Van Zandwijk JP, Bobbert MF, Baan GC, Huijing PA (1996) From twitch to tetanus: Performance of excitation dynamics optimized for a twitch in predicting tetanic muscle forces. Biol.Cybern. 75:409-417.

Wakeling J, Lee S, Arnold A, de Boef Miara M, Biewener A (2012) A muscle's force depends on the recruitment patterns of its fibers. Ann Biomed Eng 40:1708-1720.

Wakeling JM, Tijs C, Konow N, Biewener AA (2021) Modeling muscle function using experimentally determined subject-specific muscle properties. J.Biomech. 117:110242.

Walter JP, Kinney AL, Banks SA, D'Lima DD, Besier TF, Lloyd DG, Fregly BJ (2014) Muscle synergies may improve optimization prediction of knee contact forces during walking. J Biomech Eng 136:021031.

Wang J, Hamner S, Delp S, Koltun V (2012) Optimizing locomotion controllers using biologically-based actuators and objectives. ACM transactions on graphics 31:1-11.

Ward SR, Winters TM, O'Connor SM, Lieber RL (2020) Non-linear scaling of passive mechanical properties in fibers, bundles, fascicles and whole rabbit muscles. Frontiers in Physiology 11:211.

Ward SR, Eng CM, Smallwood LH, Lieber RL (2009) Are current measurements of lower extremity muscle architecture accurate? Clin.Orthop. 467:1074-1082.

Warner H, Richter H, van den Bogert, Antonie J (2020) Backstepping control of open-chain linkages actuated by antagonistic hill muscles. J. Dyn. Sys., Meas., Control 142:.

Wexler AS, Jun Ding, Binder-Macleod SA (1997) A mathematical model that predicts skeletal muscle force. TBME 44:337-348.

Wheatley BB (2020) Investigating passive muscle mechanics with biaxial stretch. Frontiers in physiology 11:1021.

Wickiewicz TL, Roy RR, Powell PL, Edgerton VR (1983) Muscle architecture of the human lower limb. Clin.Orthop. 275-283.

Widrick JJ, Stelzer JE, Shoepe TC, Garner DP (2002) Functional properties of human muscle fibers after short-term resistance exercise training. American Journal of Physiology-Regulatory, Integrative and Comparative Physiology 283:R408-R416.

Wilson C, King MA, Yeadon MR (2006) Determination of subject-specific model parameters for visco-elastic elements. Journal of Biomechanics 39:1883-1890.

Winters, J. M.,Stark, L.(1987) Biological cybernetics muscle models: What is gained and what is lost by varying model complexity. Biol. Cybern, **55**.

Winters, J. M. (1995) An improved muscle-reflex actuator for use in large-scale neuromusculoskeletal models. Annals of biomedical engineering, **23**, 359-374.

Winters, J. M. (1990) Hill-based muscle models: A systems engineering perspective. In Anonymous *Multiple Muscle Systems.* Springer, pp. 69-93.

Winters JM, Stark L (1988) Estimated mechanical properties of synergistic muscles involved in movements of a variety of human joints. Journal of biomechanics 21:1027-1041.

Winters JM, Stark L (1985) Analysis of fundamental human movement patterns through the use of in-depth antagonistic muscle models. IEEE transactions on biomedical engineering 826-839.

Winters TM, Takahashi M, Lieber RL, Ward SR (2011) Whole muscle length-tension relationships are accurately modeled as scaled sarcomeres in rabbit hindlimb muscles. J.Biomech. 44:109-115.

Wisdom KM, Delp SL, Kuhl E (2015) Use it or lose it: Multiscale skeletal muscle adaptation to mechanical stimuli. Biomechanics and modeling in mechanobiology 14:195-215.

Woittiez RD, Huijing PA, Boom H, Rozendal RH (1984) A three-dimensional muscle model: A quantified relation between form and function of skeletal muscles. J.Morphol. 182:95-113.

Wood SJ, Slater CR (2001) Safety factor at the neuromuscular junction. Prog.Neurobiol. 64:393-429.

Wyss UP, Pollak VA (1984) Surface electromyogram (EMG)/muscle force: A muscle model based on RMG peaks. Eng.Med. 13:27-33.

Xiao M, Higginson J (2010) Sensitivity of estimated muscle force in forward simulation of normal walking. Journal of applied biomechanics 26:142-149.

Young A, Stokes M, Crowe M (1984) Size and strength of the quadriceps muscles of old and young women. Eur.J.Clin.Invest. 14:282-287.

Zahalak GI (1981) A distribution-moment approximation for kinetic theories of muscular contraction. Mathematical biosciences 55:89-114.

Zajac Felix E (1989) Muscle and tendon: Properties, models, scaling, and application to biomechanics and motor control. Critical reviews in biomedical engineering 17:359-411.

Zhang Q, Fragnito N, Franz JR, Sharma N (2022) Fused ultrasound and electromyography-driven neuromuscular model to improve plantarflexion moment prediction across walking speeds.

Zhang Q, Adam NC, Hosseini Nasab SH, Taylor WR, Smith CR (2021) Techniques for in vivo measurement of ligament and tendon strain: A review. Annals of biomedical engineering 49:7-28.

Zhao M, Hollingworth S, Baylor SM (1996) Properties of tri-and tetracarboxylate Ca2 indicators in frog skeletal muscle fibers. Biophys.J. 70:896-916.

Zot HG, Hasbun JE (2016) Modeling Ca2 -bound troponin in excitation contraction coupling. Frontiers in physiology 7:406.